Real Time Biological Threat Agent Detection with a Surface Plasmon Resonance Equipped Unmanned Aerial Vehicle

Mark C. Palframan

Thesis submitted to the Faculty of the
Virginia Polytechnic Institute and State University
in partial fulfillment of the requirements for the degree of

Master of Science
in
Aerospace & Ocean Engineering

Craig A. Woolsey, Chair
David G. Schmale III
Mayuresh J. Patil

May 7, 2013
Blacksburg, Virginia

Keywords: Surface Plasmon Resonance, Unmanned Aerial Vehicle, Biological Threat Agent, Aerial Sampling, Biological Sensor

Real Time Biological Threat Agent Detection with a Surface Plasmon Resonance Equipped Unmanned Aerial Vehicle

Mark C. Palframan

A system was developed to perform real-time biological threat agent (BTA) detection with a small autonomous unmanned aerial vehicle (UAV). Biological sensors just recently reached a level of miniaturization and sensitivity that made UAV integration a feasible task. A Surface Plasmon Resonance (SPR) biosensor was integrated for the first time into a small UAV platform, allowing the UAV platform to collect and then quantify the concentration of an aerosolized biological agent in real-time. A sensor operator ran the SPR unit through a groundstation laptop and was able to wirelessly view detection results in real time. An aerial sampling mechanism was also developed for use with the SPR sensor. The collection system utilized a custom impinger setup to collect and concentrate aerosolized particles. The particles were then relocated and pressurized for use with the SPR sensor. The sampling system was tested by flying the UAV through a ground based plume of water soluble dye. During a second flight test utilizing the onboard SPR sensor, a sucrose solution was autonomously aerosolized, collected, and then detected by the combined sampling and SPR sensor subsystems, validating the system's functionality. The real-time BTA detection system has paved the way for future work quantifying biological agents in the atmosphere and performing source localization procedures.

This work was partially sponsored by the Institute for Critical Technology and Applied Science at Virginia Tech.

Acknowledgments

First off, I would like to thank my advisor, Dr. Craig Woolsey, for his continued mentorship and assistance with my graduate studies. When Dr. Woolsey first approached me with the opportunity to work on this project, I was unaware of how much of a learning experience it would be. With his guidance, I was first introduced to the world UAVs, to which I quickly became enamored. I am especially appreciative of Dr. Woolsey's consistent positive outlook despite several setbacks during flight activities.

I would also like to thank my co-advisor, Dr. David Schmale, for his help and insight into aerobiological sampling. Dr. Schmale's contributions and guidance helped to shape the aerobiological collection system design in addition to formulating plans for effective and comprehensive flight testing. Dr. Schmale also assisted in flight tests as a legal observer.

The SPR portion of this project would not have been possible if not for the members of the the Schmale Laboratory, in particular, Hope Gruszewski and Piyum Khatibi, who worked tirelessly to prepare the SPR sensor for flight activities. Thanks also to Dr. Dash Gantulga for her assistance in setting up dye quantification procedures.

John Cianchetti was an invaluable member of the project. Flight activities would not have been possible without John's continued mentorship and unwavering dedication. John's contributions ranged from the design of the aerial spray system, preparation of the SPAARO airframes, and piloting flight tests. I would also like to acknowledge John Coggin for volunteering his time to pilot and help with flight tests.

Special thanks to the members of the Nonlinear Systems Lab for their assistance in flight activities, especially Ony Arifianto, Lawrence Hale, and Jeff Garnand-Royo for serving as observers and ground station operators. Last but not least, I would like to thank my friends and family for their continuous support.

Contents

List of Figures

List of Tables

Chapter 1

Introduction

Small unmanned aerial vehicles (UAVs) have been successfully used to detect airborne biota, such as fungal spores, with a variety of sampling techniques. However, these methods generally required samples to be post-processed in a lab to confirm a detection result [1, 2, 3]. The capability to perform real-time detection of biological threat agents (BTAs) by a small UAV would make adaptive aerial sampling feasible and enable the UAV to quickly characterize a biological release event, allowing for a more immediate and informed response.

BTAs, which include bacteria, toxins, and viruses, remain a serious threat to both civilian and military populations [4]. A small UAV that could detect BTAs in near real-time would have a number of potential applications. For example, the ability to detect and quantify environmental pollutants could lead to faster toxic waste cleanup as well as improved risk assessment procedures for human exposure in affected areas. An integrated

biosensor platform would also eliminate the need to transport samples to a laboratory for processing, cutting down on expense, notification time, and other logistical complications in harsh environments [5]. Fast response time is essential for reacting to events ranging from localized spore tracking to large contaminant, improving our ability to contain and predict the spread of such events [6]. In recent studies, various BTAs have been shown to travel great distances through the atmospheric boundary layer in short amounts of time, underscoring the importance of response time [3]. An anthrax attack simulation conducted by Wein et al. showed that an improved detection time would directly result in a lower fatality rate given a release near a populated area [7]. In the case of such an attack, the ability to detect several BTAs in parallel would characterize the nature of an emergency within minutes, focusing response efforts, reducing response costs to civilian organizations, and allowing for prompt diagnosis and treatment of exposed victims [8].

This thesis presents the the results of a multi-step process leading up to a fully autonomous aerial collection system with Surface Plasmon Resonance (SPR) detection. This process is outlined in Figure 1.1, where all items except for the "Spray and Capture SPR Flight Test" discussed in Section 6 have been completed. Section 2 will first discuss the history of biological sensing with UAVs along with the principals of SPR operation. The design and integration of an aerial collection system will then be discussed, where a system was implemented into a UAV platform for sampling aerosolized particles in the air. The design of a parallel objective system, an aerial spray system to be implemented on a small UAV platform, will also be discussed. Next, a protocol for obtaining quantitative concentration

data from flight tests is discussed in Section 4. Section 5 will then present te results from each of the ground and flight tests seen in Figure 1.1. The aerial spray system flight test confirmed the practicality of the spray system design, the dye plume flight test validated the design of the collection subsystem as well as determined the collection efficiency, and the SPR ground and flight experiments tested the integrated SPR portion of the aerial collection and detection system.

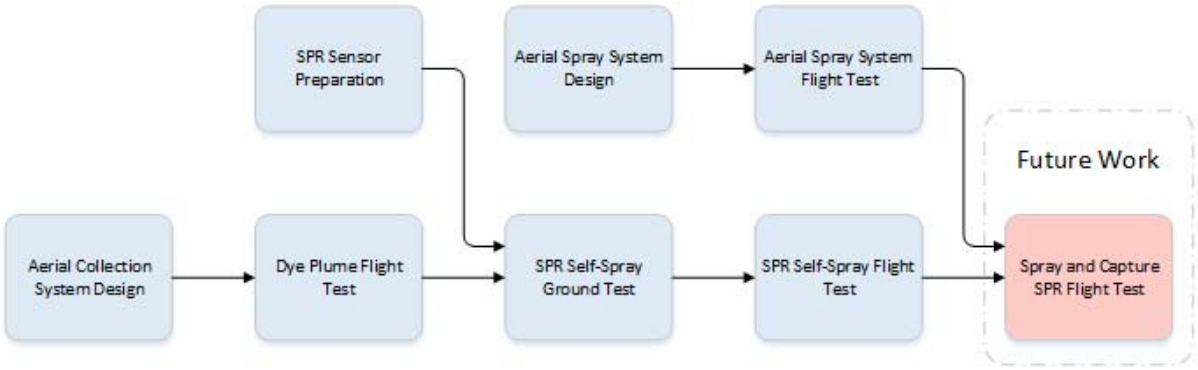

Figure 1.1: The SPR based aerial collection system integration has been broken down into several stages. All items in blue boxes are discussed in this paper, with the red box containing future work.

Chapter 2

Background Information

2.1 Biological Sensors

Over the last half century, several techniques have been utilized for the detection of biological agents. These methods varied in terms of sensor types (optical, chemical, etc.), detection times, minimum detection concentrations, and accuracies. Developed in 1971, Enzyme Linked Immunoabsorbant Assays (ELISAs) were the first streamlined procedures to use enzymes for detection as opposed to radioactive labels. These ELISAs were highly accurate, highly sensitive assays that could detect and quantify BTAs in a laboratory environment over the course of several hours [6]. While accuracy and sensitivity were desired characteristics for biological sensors, the slow response time of ELISAs made them impractical for small UAV deployment. Another approach, an optical based sensor using immunomagnetic separation

coupled with electro-chemiluminescence and fluorescence (IMSECL/FCL), yielded a significantly reduced detection time of just 30 minutes [8]. Advances in an alternate technique, Rapid Chromatograph Assays (RCAs), have brought detection times down even lower, successfully detecting an analyte in just 15 minutes while also maintaining a high sensitivity [4]. Following the development of RCAs, Flourescance Array Biosensensors were shown to detect multiple agents simultaneously with a response time of 14 minutes, and a fairly low detection limit of only 10^5 cfu/mL [9]. These detection times made these sensors much more reasonable for integration when considering the flight time of modern small UAVs.

2.2 Biological Sampling with UAVs

Small UAVs are uniquely suited to the task of biological sampling. Besides their flexibility and maneuverability, these UAVs can quickly sample massive volumes of air. Aided by their natural air speed, this large amount of sampled air allows UAVs to detect low concentrations of sparsely distributed constituents. Both increasing the airspeed of the UAV by a factor of V_i or increasing the sampling time by a factor of t_f results in an increased collected sample concentration. In fact, if there is an even distribution of contaminant in the air, a UAV can detect concentrations of contaminants a factor of $V_i \times t_i$ smaller than it previously could.

Small UAVs have been successfully used to detect biological substances using a variety of methods. Schmale et al. used UAVs with custom petri plate samplers to track *Phytophthora*

infestans (potato late blight) as it spread from field to field [1, 3]. Schmale has also used an ionic spore trap integrated into a small UAV platform for aerobiological sampling. Anderson et al. used a fiberoptic immunoassay biosensor integrated into a small UAV platform to detect plumes of *Bacillus globigii* released on the ground [2, 10]. Naimushin used a full-scale Rutan VariViggen aircraft as a surrogate UAV platform in conjunction with an SPR sensor. The SPR sensor was able to detect and analyze aerosolized ovalbumin and horseradish peroxide sprayed from an external release port on the vehicle [11].

2.3 Surface Plasmon Resonance Sensors

Since being first developed for gas detection and biosensing by Bo Liedberg in 1983, SPR sensors have been been used consistently for biodetection in a laboratory setting [11, 12, 13]. SPR sensors can detect a wide variety of analytes, including pathogenic bacteria, protein toxins, and small molecules.

2.3.1 Principles of Operation

Surface Plasmon Polaritons (SPPs) are "electromagnetic waves coupled with charge oscillations of free electrons in a metal and dielectric medium" as defined by Roh et al. [13]. In an SPR device, a photon coupled with an SPP propagate along the surface of a gold plate as an electromagnetic wave at a particular eigenfrequency. When SPPs are optically induced, their resulting eigenfrequencies can be observed and measured, forming the basic principal

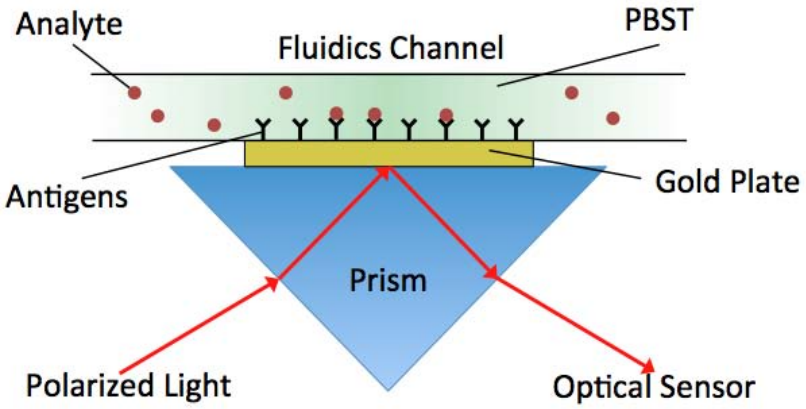

Figure 2.1: As analyte and PBST flow through the fluidics channel in the SPR sensor, analyte binds to the antigens goading the gold plate. The resulting resonance response changes the reflection angle of the polarized light ray shining through the prism on the underside of the gold plate. This change in reflection angle is then measured by an optical sensor.

for detection by SPR sensors. The Spreeta 2000 chip utilizes the standard Kretschmann configuration with prism coupling, where a ray of monochromatic light is shone though a glass prism and reflected off of a 50nm gold plate, as in Figure 2.1 [13]. The opposite side of the gold plate is coated and processed in a laboratory with specific antibodies for the detection of a corresponding analyte. In the SPIRIT system, a fluidic channel passes over the non-prism side of the gold plates of four Spreeta chips in series. As a biological sample suspended in a Phosphate Buffered Saline + 0.1% Tween 20 (PBST) solution flows through the fluidic channel and across each plate, analyte continuously bonds, or associates, and dissociates from the plate antibodies until a steady state is reached. When the gold plates are induced by a the polarized light ray, the resulting surface plasmon resonance shifts the reflection angle of the light, which is then measured by an optical sensor in terms of resonance units (RUs). The RU value can be converted to an analyte concentration. 1000

RUs is approximately equal to 0.1°, where the angle shift is directly proportional to the concentration of analytes in the sensor's fluidic channel [14]. Because SPR does not require a tracker, such as a fluorescent material to mark each analyte, to be bound in a two-site noncompetitive immunoassay arrangement, all analytes will have a free bind site available. Taking advantage of this, an "amplifier" of additional antibodies can be injected into the flow to bond to the open sites and amplify the response, which reduces false readings, increases concentration accuracy, and lowers the minimum detection threshold.

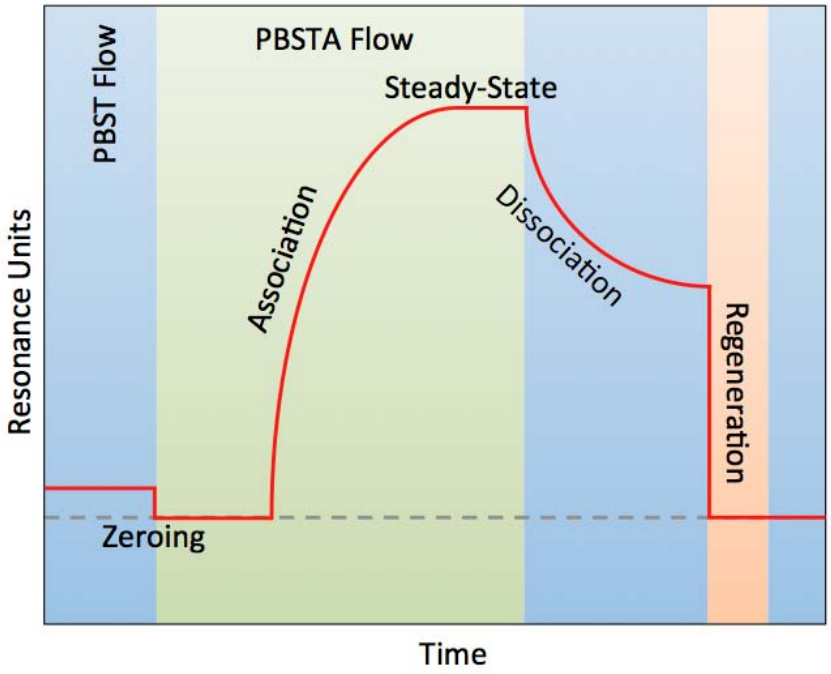

Figure 2.2: The SPR sensor response is initially zeroed during PBST flow. Analyte then binds to the gold plate during association phase of PBSTA flow. The steady-state RU value during PBSTA flow is used to determine the analyte concentration. When PBST flow resumes, analyte begins to dissociate from the gold plate. The injection of a regeneration solution completes the process of clearing analyte out of the sensor chamber and the sensor response returns to a value of zero.

Figure 2.2 shows what the resultant graph from a single Spreeta chip detection might

look like. Buffer first flows through the sensor to initialize it until the RU value reaches a steady-state [14]. The system is then "zeroed" and the previously measured RU value is subtracted from all future readings so that any RU value above zero reflects a detected concentration. Next, sample is injected into the buffer solution and association begins as the buffer/sample flows across the binding area on the gold plate. The RU will eventually level off as the system reaches a steady-state, where analyte is associating and dissociating at the same rate. Since resonance is directly proportional to the analyte concentration, the RU measurement at this steady-state region can then converted to a concentration value based on laboratory-generated calibration data. If the flow rate is not sufficiently fast, RU will rise but not reach a steady state, and only a lower concentration limit can be determined from the resulting curve. When the injection of sample is completed, dissociation occurs, where analyte-antigen bonds slowly break down. Dissociation results in an asymptotic decrease in RU, which will likely not reach the "zeroed" mark. Therefore a regenerative solution may be injected in order to "clean" the sensor and prepare it for further detections.

2.3.2 Sensor Advantages

Biosensor technology had just recently reached a level where it can be incorporated into a small UAV airframe. In a purely physical sense, smaller and lighter weight biosensors could now fit into the payload bay of a small UAV. Several companies including Biacore Life Sciences, Lecia Mirosystems, GWC Technologies, IBIS Technologies, and Toyobo Co., Ltd have developed SPR sensor systems, although they proved too large and heavy to be

used with a small UAV platform [15]. The Spreeta 2000 sensor chip, however, was ideal for use in a small aerial system, as it is compact, rugged, robust, and inexpensive [15]. Developed in the 1990s by Texas Instruments Inc., the Spreeta chip is roughly the size of a US dime. The decreased sensor weight of the Spreeta system will allow small UAVs to exhibit longer flight times with these sensors, which, coupled with increasingly lower detection times, will result in more detection events per flight. The Spreeta based SPIRIT (Surface Plasmon Instrumentation for the Rapid Identification of Toxins) biosensor from Seattle Sensors, shown in Figure 2.3, was eventually chosen to be used in our experiments. The SPIRIT system had proven itself with analyte detection both in a laboratory setting [15] and while aboard Naimushin's full scale surrogate UAV [11].

In recent years SPR technology has advanced to the point where it is no longer limited by low sensitivities, slow response times, and single sample sizes [4]. Traditionally when used in the field, a high airborne-particle-count trigger would be used to determine whether or not a biological plume was present, and would then lead to the initiation a biological detection procedure. The ability to easily take repeated samples would reduce reliance on these triggers, and allow for repeatable, faster, and multi-sample sensors, such as an SPR sensor, to be much more applicable for use in areas with consistently elevated particle counts, such as disaster areas and warzones [4].

The Analyte 2000 biosensor flown by Anderson et al. utilized evanescent wave spectroscopy with a tapered fiberoptic probe to measure specific antigens with a 10^6 cfu/mL sensitivity [10]. The SPIRIT SPR system, however, offered many advantages over the Ana-

Figure 2.3: The SPIRIT SPR sensor system was originally designed to be used as a rugged mobile field unit. Photo courtesy of Mark C. Palframan.

lyte 2000 but had yet to be integrated into a UAV platform [2]. In addition to its compact size and light weight, the SPIRIT SPR system had a significantly reduced lower bound sensitivity of 100-1000 cfu/mL, allowing it to detect smaller concentrations of analyte in the air. The SPIRIT system allowed for a 6 minute response time and continuous real time monitoring of detected concentrations. Unlike light addressable potentiometric sensors, ELISA, IMS-ECL, FCL, RCA, and others, SPR doesn't consume any regents during detection, and can wash out any remaining analyte after detection with a regenerative solution. This allowed the SPIRIT system to do repeated detection cycles with minimal preparation time in-between samples [11]. The four Spreeta chips in the SPIRIT system allowed for either

redundant detection, detection of up to three different analytes (with the fourth chip acting as a control), or the detection of complex molecules, making it a very flexible sensor system.

Chapter 3

Experimental Setup

3.1 Aerial Platforms

Two aerial platforms were used during these experiments. A SPAARO (Small Platform for Autonomous Aerial Research Operations) airframe was used for it's ability to carry large heavy payloads, and a Sig Rascal 110 was used for it's maneuverability.

3.1.1 SPAARO

The Virginia Tech Nonlinear Systems Lab's SPAARO (Figure 3.1) was chosen as the sensor carrying aircraft [16, 17, 18]. Similar to the manned VariViggen used by Naimushin et al., SPAARO featured a pusher-style propeller, which allowed the sampler inlet to be located at the front of the plane where it was free from engine contaminants and air mixing

from the propellor [11]. With a 12 foot wingspan and a 7.5 hp engine, SPAARO could lift a 12 lb payload in its large 1.75' X 1' X 0.5' payload bay. This allowed the SPIRIT and aerial collection systems to be comfortably mounted in an easily accessible location. SPAARO was instrumented with a Piccolo II autopilot from Cloud Cap Technology, a Novatell DGPS receiver, and a SpaceAge Control air data probe for pitot-static, angle of attack, and side slip angle measurements. Inflight data was also measured and logged using an Eagle Tree Systems Seagull Wireless Telemetry unit, as the Piccolo system was subject to export control under International Trade and Arms Regulations (ITAR), making it necessary to employ a separate sensing system for data reporting. In addition to the autopilot groundstation, SPAARO maintained inflight connectivity with a laptop on the ground via a wireless RS-232 connection using a MaxStream XTend-PKG RF Modem to control and view data from the SPR sensor in real time.

3.1.2 Sig Rascal

Sig Rascal 110s, commercially available sport airframes, were used during some initial testing. The Rascals were slightly modified with either external brackets to accommodate an aerial spray system, or petri plate samplers, as seen in Figure 3.2 and discussed in more detail in Section 3.4.1. All Rascals in these experiments were flown manually without autopilot control or additional telemetry.

Figure 3.1: Virginia Tech's SPAARO airframe at Kentland Research Farm, Virginia. Photo courtesy of Mark C. Palframan.

3.2 Flight Locations

Local flights were conducted at the KEAS (Kentland Experimental Aerial Systems) Labratory, located on Virginia Tech's Kentland Research Farm (Figure 3.3). The KEAS Lab featured a paved 70 by 300 ft UAV runway located amongst agricultural fields. All SPAARO airframes were flown under Certificate Of Authorization (COA) numbers 2011-ESA-64 and 2012-ESA-92.

Offsite test flights were conducted in restricted airspace in Fort Pickett, Virginia, seen in Figure 3.4.

Figure 3.2: A Sig Rascal 110 in flight with closed petri plate samplers seen on the leading edge of each wing. Photo courtesy of Mark C. Palframan.

3.3 Aerial Spray System

The aerial spray system used a three liter pressurized container connected to two spray heads which were attached at the rear of the plane. The sprayer system was originally installed and tested by mounting the pressurized canister on the underside of a Sig Rascal airframe. The Rascal was found to exhibit undesirable flight characteristics due to the heavy weight and altered CG location. No spray was released during this test, as aerial release is restricted by the Federal Aviation Administration (FAA). When the system was installed on SPAARO, the canister was able to fit inside the payload bay instead of being mounted on the exterior of the plane. This, in combination with the increased payload carrying capacity of SPAARO, allowed the plane to remain balanced with either a full or empty canister and exhibit no detectable effect on the UAV's flying qualities as a result of the externally mounted spray lines. SPAARO was therefore chosen to be used as the airframe for all aerial spray

Figure 3.3: The KEAS UAV runway located at Virginia Tech's Kentland Farm served as a base of operations for local flight activities. Photo courtesy of Mark C. Palframan.

flight operations.

To operate the system, the main canister was filled with the desired amount of liquid and then pressurized through a one way valve using a bicycle pump. The spray release was controlled by a servo-actuated solenoid valve that could be triggered by either the primary or secondary pilot of the associated airframe. Inside of the pressure vessel, the solenoid was connected to a clunk to ensure a constant stream of liquid was drawn out. From the solenoid, the spray tubing was split and run along the aircraft's dual tail booms, where each tube ended in a misting spray head. Figure 3.4 shows the sprayer system being tested after installation on SPAARO.

Figure 3.4: The aerial spray system is tested on the ground with a blue dye before flight at Fort Pickett in Blackstone, Virginia. The two spray lines can be seen attached to the underside of the tail booms. Photo courtesy of Mark C. Palframan.

3.4 Sample Collection System

Before being processed by the SPR sensor itself, airborne particles had to be collected from the surrounding air and processed into a form usable by the sensor. Designed for in-the-field and benchtop laboratory experiments, the SPIRIT system introduces a sample into its fluidics system through a special inlet port. Sample was delivered through the injection port via a syringe of concentrated analyte. Once inside the sensor unit, the sample was mixed with a solution of PBST before being transferred through the Spreeta SPR chips for analysis. This injection system presented two immediate problems, first that the analyte would need to be highly concentrated in order to get a reading above the minimum detection limit, and secondly that the analyte would need to be autonomously drawn into and subsequently dispensed from a syringe. Naimushin et al. solved these problems by using a gravity droplet collector to both collect and concentrate the sample and then transfer the sample from the

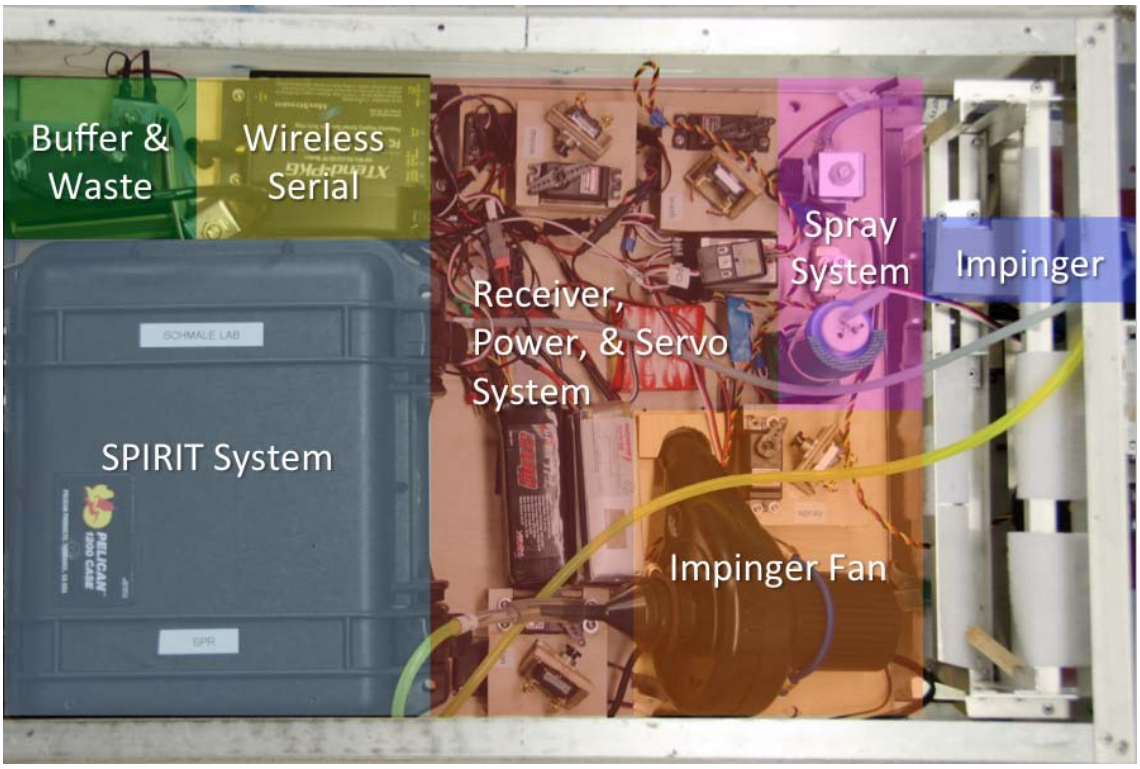

Figure 3.5: The SPR and aerial collection sub systems can be seen in SPAARO's payload bay with the top removed. Photo courtesy of Mark C. Palframan.

collector to the modified SPR system using an onboard sensor operator [11]. A gravity droplet collector system was deemed implausible for integration into the SPAARO UAV as it was a large and heavy system relative to the size and weight of the UAV. In order to overcome these obstacles, a custom semi-autonomous aerial sample collection system, seen in Figure 3.5, was developed for use with the SPIRIT system.

3.4.1 Filter Paper Samplers

Petri plate aerobiological samplers have been used with much success in the past on Senior Telemaster, Sig Rascal, and SPAARO airframes [1, 3, 19, 20, 21]. To commence

Figure 3.6: Petri plate samplers on the underside of SPAARO open (left) and closed (right). The filter papers can be seen to be blue after capturing blue dye particles in flight. Photos courtesy of Mark C. Palframan.

sampling, servos simultaneously swung two petri plates out perpendicular to the air flow, and closed them again when sampling was complete, as seen in Figure 3.6. When closed, the petri plates mated with their corresponding cover plates to reduce sample contamination. While traditionally filled with a biological medium designed to grow microbes or fungal spores after collection, our petri plate samplers used 3.5 inch diameter filter papers in order to collect dyed liquid particles in the air [3].

3.4.2 Sampler End Cap

In order to regulate air flow into the collection tube, a servo operated end cap, seen in Figure 3.7, was opened at the start of each sampling cycle, and closed immediately following the wash cycle.

Figure 3.7: The servo operated sampler end cap his shown open for sampling (left) and then closed (right). The misting spray head can also be seen in front of the collection tube opening, while tubing for the recirculating wash mechanism can be seen on the outside of the collection tube. Photos courtesy of Mark C. Palframan.

3.4.3 Impinger

The airborne particle collector design was centered around an air sampling impinger, in which aerosolized particles in the air were captured by being impacted into a solution of PBST. The impinger, shown in Figure 3.8, used a combination of ram air and a downstream fan to create a pressure gradient which forced the "sampled" air to bubble through the PBST solution. Heavier airborne particles, including the biological agents to be sensed with the SPR, remained in the PBST solution as the "sampled" air was pulled through a downstream fan and released through a vent on the underside of the aircraft. The servo operated end cap opened to allow air to flow into the sampling tube when the fan was turned on. Upstream of the end cap, a spray nozzle, which can be seen in Figure 3.7, seeded the flow from a servo operated syringe containing the analyte. By collecting the sample directly in the

buffer solution, we solved both injection issues simultaneously, as we no longer needed to pre-concentrate the analyte, or inject it via syringe.

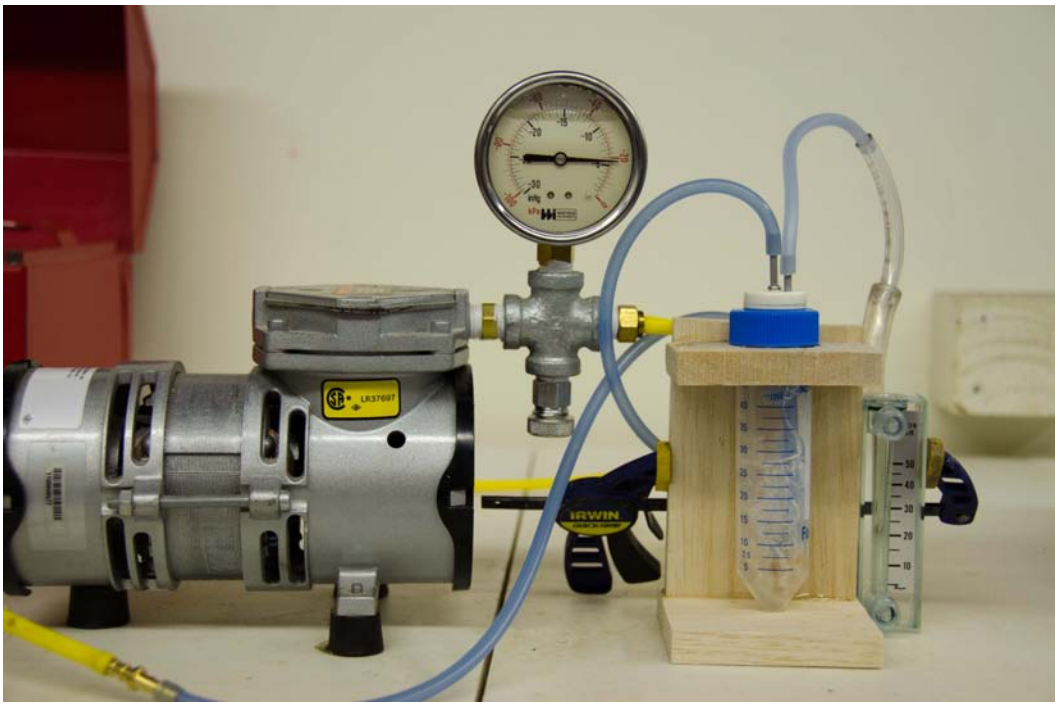

Figure 3.8: Water is bubbled through the impinger vial with a compressor pump pulling 20 kPa to test the impinger system. Photo courtesy of Mark C. Palframan.

3.4.4 Fluidics

The impinger setup was tested by using an external fan to simulate a cruising airspeed of approximately $70\,{}^{ft}/_{s}$. Figure 3.10 shows how the collection tube was funneled into the impinger, while the downstream fan created a further pressure gradient. Spray was released both from a distance in front of the collection tube to represent plume sampling and in a "self-spray" configuration like that used in Section 5.3 and also shown in Figure 3.7. In the case of Figure 3.10, dyed mist was released directly into the collection tube via a solenoid regulated

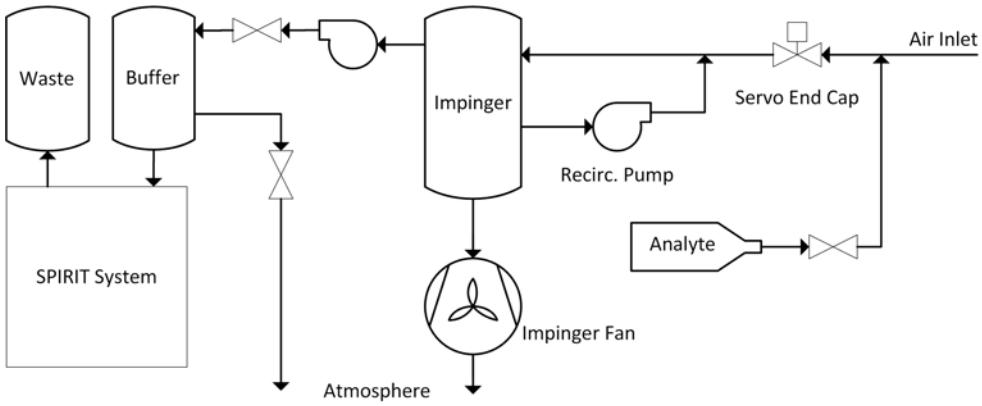

Figure 3.9: Analyte from the self spray mechanism was first captured in the impinger vial. The impinger fan was then turned off and the recirculation pump was used to wash the walls of the collection tube, with the sample then settling back into the impinger vial. When the two solenoids surrounding the buffer reservoir were opened, a second pump moved the sample from the impinger to the buffer reservoir, from which it was drawn into the SPIRIT system, and then deposited in the waste container.

pressure vessel. It can be clearly seen that many particles were caught on the side of the tube before reaching the impinger. In order to get an accurate concentration reading, a majority of particles in the sampled air needed to reach the SPR sensor. To improve upon this, the sampling tube was shortened and widened in further iterations of the design. To facilitate the capture of particles that still ended up on the tube walls, a recirculation pump was used to wash the walls of the sampling tube with the PBST and analyte solution (PBSTA) from the impinger vial following the air sampling phase. In addition, the wash mechanism also served to trip the boundary layer on the inside of the collection tube. Following the sampling and washing, the PBSTA solution was pumped to the buffer reservoir attached to the SPIRIT system and subsequently pressurized by the SPIRIT system after solenoids located on the inlet and outlet to the buffer reservoir (see Figure 3.9) were closed. This pressurization served to remove any bubbles that might have interfered with sensor readings, replacing the

debubbling phase implemented by Naimushin [11].

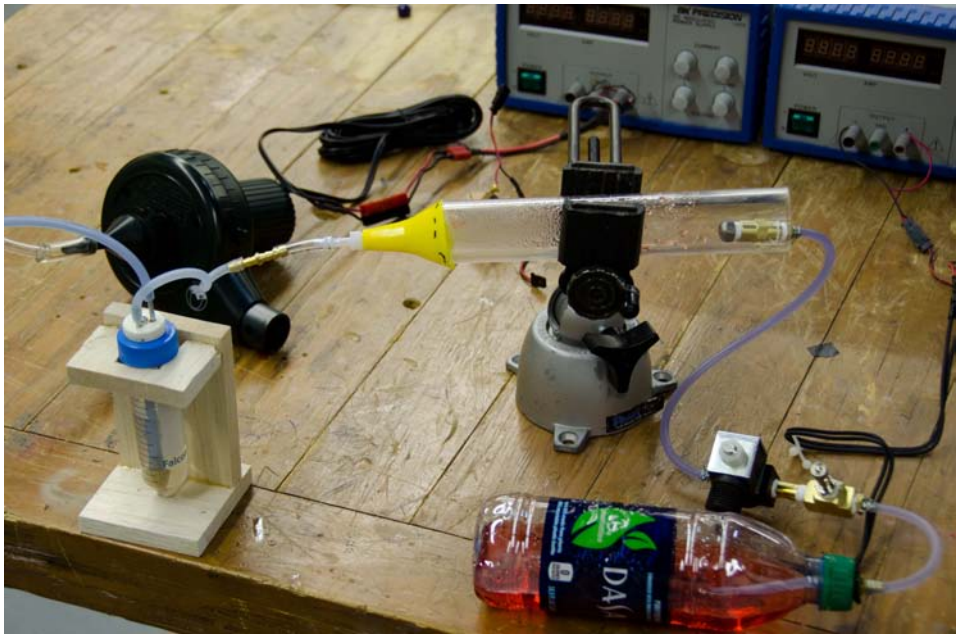

Figure 3.10: Dyed water was sprayed directly into the collection tube leading into the impinger from a solenoid controlled pressure vessel. The red liquid can be seen on the walls of the collection tube. Photo courtesy of Mark C. Palframan.

3.4.5 SPIRIT Integration

The buffer and waste vials were mounted externally to the SPIRIT casing to allow them to remain vertical during flight. Three small holes were drilled in the casing to allow the power line, RS-232 connector, and fluidics lines to integrate with the SPR. As previously mentioned, the buffer reservoir was modified with an additional line in and out through two separate solenoids in order to allow the PBSTA solution to enter the reservoir. Because of this PBSTA solution, there was no pure buffer to flow through the Spreeta chips to initialize the system, therefore the SPR needed to be zeroed prior to takeoff. There was not a traditional

dissociation phase, and dissociation did not take place until the buffer reservoir was emptied and replaced with pure PBST. As the system was set up to take a single sample, there also was not a surface regeneration phase while in the air.

3.4.6 Automation

An Arduino Mega 1280 micro controller (Figure 3.11) was used to automate and regulate the various collector processes for the three sampling missions. Relays were used to control the recirculation pump, relocation pump, solenoids, and impinger fan, while pulse-width modulated (PWM) signals were used to control all servo operated members. A PWM signal from the main SPAARO receiver was also linked to the Arduino board, allowing the entire system to be triggered by either the pilot or backup pilot's transmitter. The various sampling phases can be seen below. The code that was implemented on the Arduino can be found in Appendix D.

1. Initialization
    (a) Servo operated end cap is opened
    (b) Impinger fan is turned on
    (c) Petri plate samplers are opened†
2. Sampling Phase
    (a) Spray solenoid is opened‡
    (b) Spray solenoid is closed‡
3. Wash Cycle
    (a) Recirculation pump is turned on

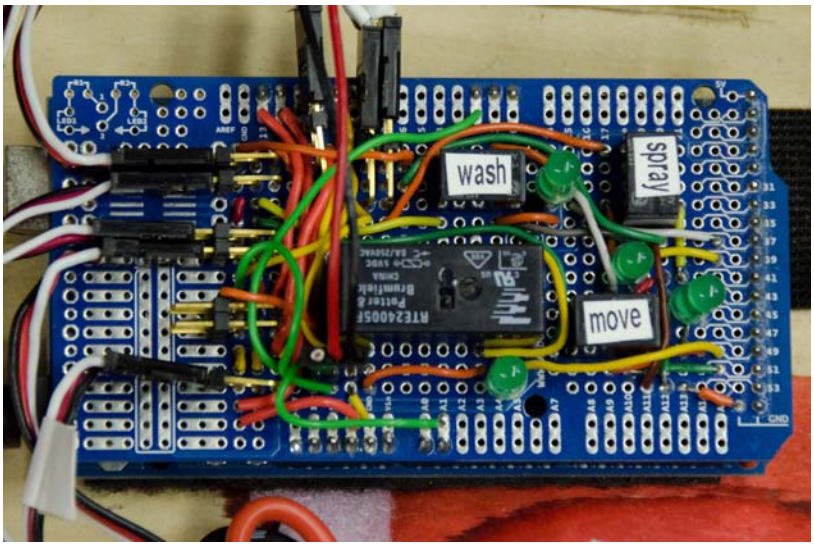

Figure 3.11: The SPRduino system outputs PWM signals to controller servomotors and uses relays to regulate voltage to the remaining collection system components. LEDs mounted to the board also light up when their corresponding relays are active. Photo courtesy of Mark C. Palframan.

4. Finish Sampling
    (a) Recirculation pump is turned off
    (b) Servo operated end cap is closed
    (c) Impinger fan is turned off
    (d) Petri plate samplers are closed†
5. Relocation Cycle
    (a) Buffer reservoir solenoids are opened
    (b) Buffer reservoir pump is turned on
    (c) Buffer reservoir pump is turned off
    (d) Buffer reservoir solenoids are closed
    (e) Reservoir pressurization commences

†Dye Plume Flight Test Only

‡Self-Spray Flight Test Only

Chapter 4

Dye Quantification

Southern States SureMark blue colorant was used during flight testing as a surrogate for a biological medium. This allowed a large number of concentrations to be quickly and accurately quantified in the lab. This also cut down the use of biological material, which was found to be prohibitively expensive for spraying in large quantities.

A dye calibration curve was generated using a spectrophotometer to quantify dye concentrations at $640\,nm$ in terms of Optical Density (OD). Dye was mixed in various concentrations of water and Dye Units (DUs) to produce 3 parallel $1\,ml$ samples per concentration. These samples were then run through the spectrophotometer to produce the calibration curve seen in Figure 4.1. The resultant trend line of $OD = 0.0469\,DU$ has an R^2 value of 0.96. The associated spectrophotometer values can be found in Table A.2.

In experiments, dye collected in liquid form, either from a spray reservoir or straight from

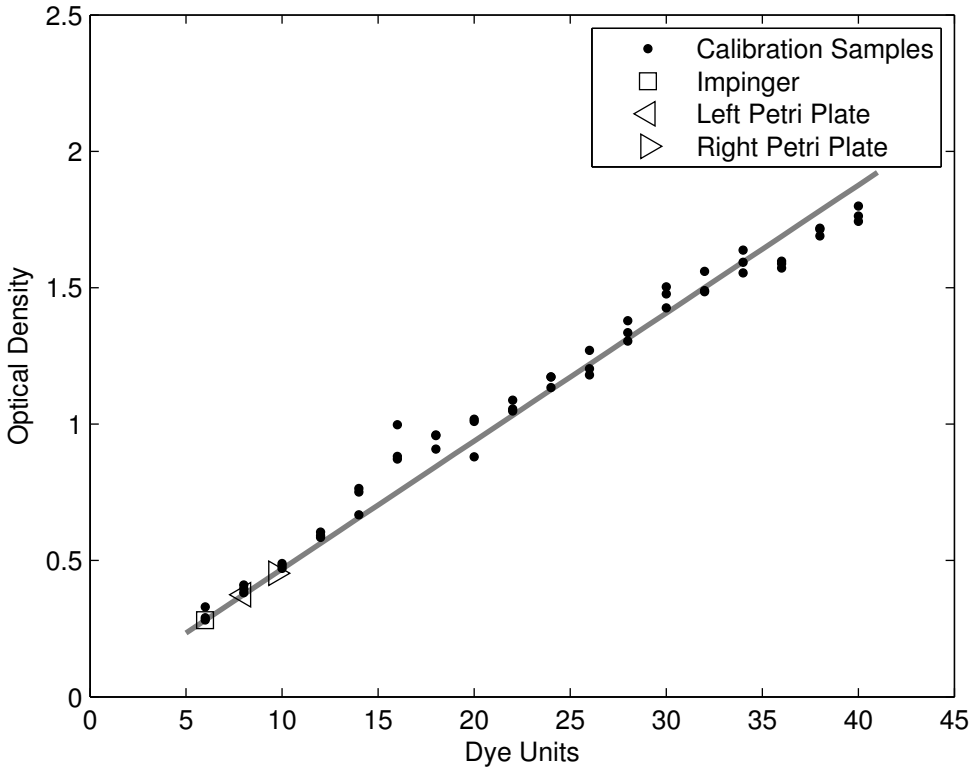

Figure 4.1: The dye calibration curve was generated using 3 redundant samples at each of 18 concentrations. The resultant curve, shown in blue, has an R^2 value of 0.96. The curve was used to calculate the dye concentration of filter paper and impinger samples from UAV test flights. The filter paper samples and impinger sample can be seen on the calibration curve as green circles and a blue triangle, respectively.

the impinger, could easily be quantified by again running 3 parallel $1\,ml$ samples through the spectrophotometer and backing out the Dye Units as $DU = 21.32\,OD$. Flight test values can also be seen in Figure 4.1.

Dye collected with filter paper was quantified using the process shown in Figure 4.2. Dyed filter papers were first cut into quarters before being placed in a $50\,ml$ tube with $5\,ml$ of DI water. The samples were mixed for 20 minutes with a Clay Adams Nutator Orbital Mixer, flipping the samples over after 10 minutes. Samples were then centrifuged for 2 minutes at 1000 g's to remove all liquid from the filter papers. The now fully liquid samples were then processed with the spectrophotometer as before.

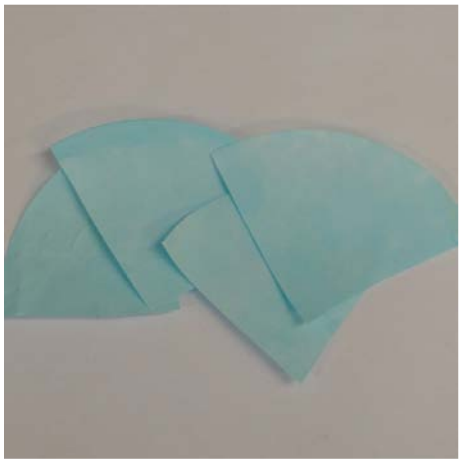

(a) Filter papers are cut into quarters

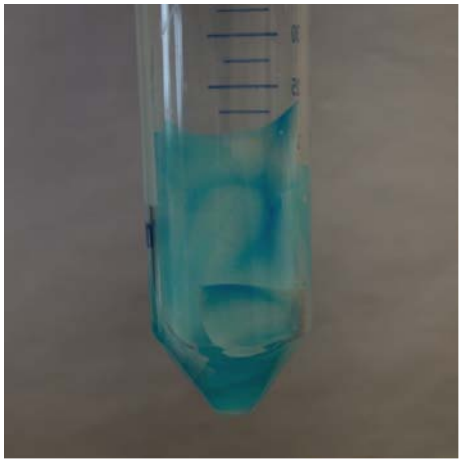

(b) Papers are submerged in water

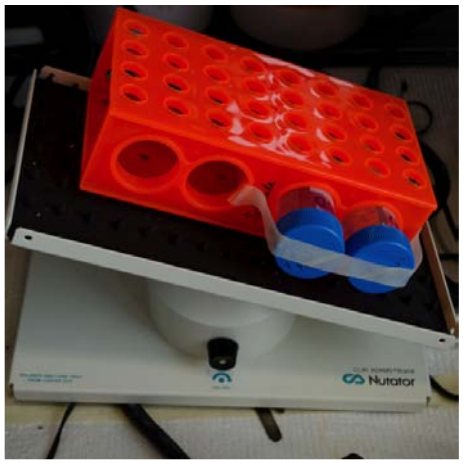

(c) Samples are mixed with a rotating shaker

(d) Sample before centrifuging

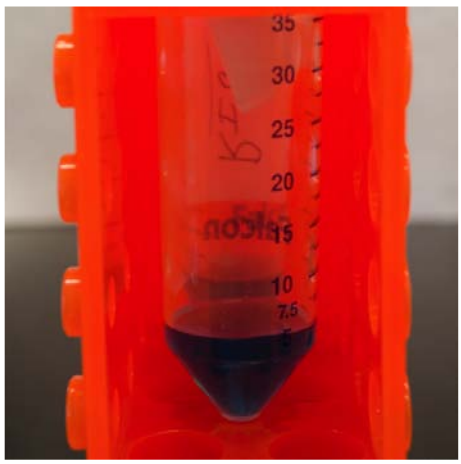

(e) Centrifuged sample

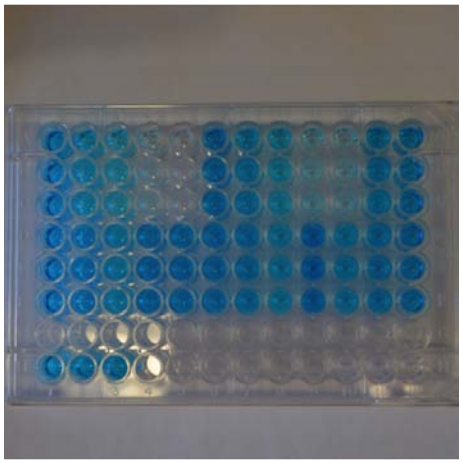

(f) Spectrophotometer test plate

Figure 4.2: A dye quantification process was developed in order to calculate the concentration of blue dye collected by filter paper samples. Photos courtesy of Mark C. Palframan.

Chapter 5

Results

5.1 Aerial Spray System Flight Test

In order to test the dispersion and effectiveness of the aerial spray system, a Sig Rascal was used to collect spray by flying behind a SPAARO airframe equipped with the aerial spray system in unrestricted airspace at Fort Pickett, Virginia. The SPAARO was put into an autonomous racetrack flight pattern while the Rascal, equipped with filter paper petri dish samplers (Figure 3.2), was manually flown in coordination behind the sprayer plane. The spray canister was filled with a mixture of water and blue colorant and then pressurized with a bicycle pump. The sprayer released several ten second bursts of dye which were captured by the Rascal's petri plate samplers.

Upon investigation after landing, the Rascal's filter paper samplers, seen in Figure 5.1,

had successfully collected dye from the sprayer plane. This result served as a proof of concept that an SPR equipped SPAARO could collect biological agent sprayed from another SPAARO unit. This would allow an aero-biological sampling and detection test to be performed while only using a minimal amount of biological reagent.

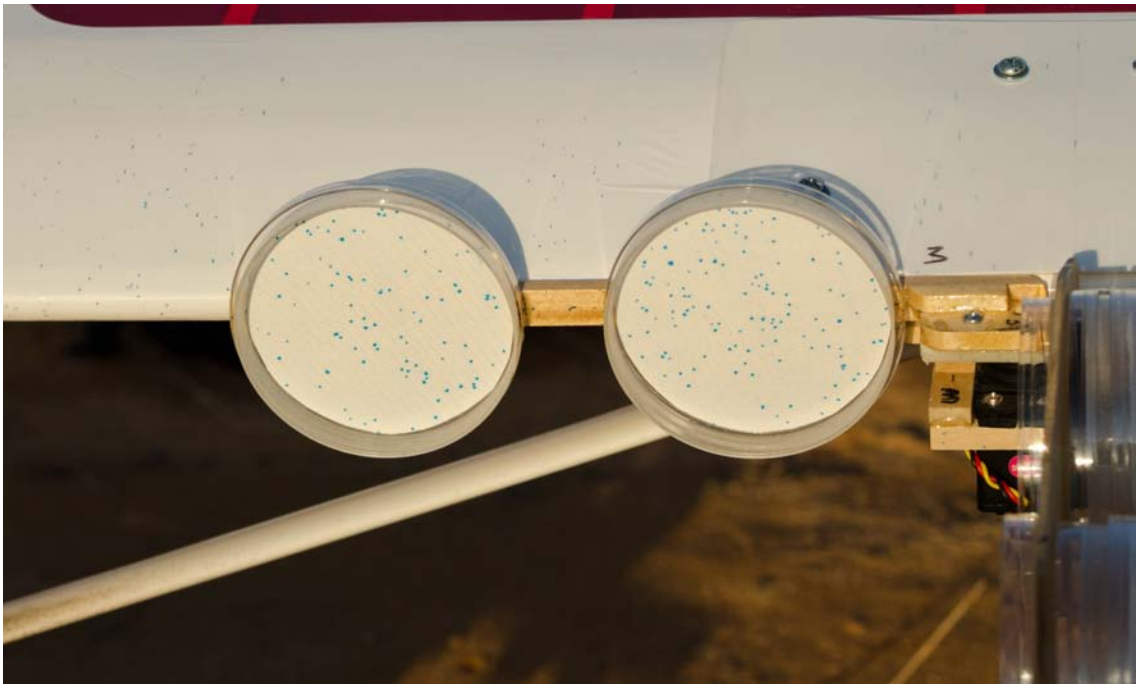

Figure 5.1: A Sig Rascal's airframe with wing mounted filter paper petri samplers was flown behind a SPAARO UAV releasing misted blue dye at Fort Pickett in Blackstone, Virginia. Spots of blue dye were found on the filter paper samples as well as on the leading edge of the wing. Photo courtesy of Mark C. Palframan.

5.2 Dye Plume Flight Test

In order to determine the efficiency of the collection system, a SPAARO airframe (without the SPR system on board) was flown through a plume of dye generated at ground level, collecting the dye with both the petri plate samplers and the impinger system (Figure 5.2).

Both samples were then analyzed and compared in the lab as per Chapter 4.

Figure 5.2: SPAARO flew through and collected samples from a plume of dyed water generated by an orchard sprayer at Virginia Tech's Kentland Farm facility. Photo courtesy of Mark C. Palframan.

5.2.1 Setup and Flight Path

An orchard sprayer at Virginia Tech's Kentland Research Farm, shown in Figure 5.3, was filled with 100 gallons of water/dye mixture at 2460 $^{DU}/_{gal}$ and set up to release spray in the downwind direction. An array of petri plates with filter papers were set up in a semicircle behind the the orchard sprayer to characterize the dispersion of the plume. The plates were placed at even angular intervals and five foot radial intervals, as seen in Figure 5.4a. The array was set up such that the wind was blowing in the positive X direction according to the figure.

The filter paper samples from the array, which can be seen in Figure 5.5, were processed

Figure 5.3: An semicircle array of petri dishes containing filter papers was placed around an orchard sprayer. The filter papers collected samples from the orchard sprayer plume which were later used to characterize the plume distribution. Photo courtesy of Mark C. Palframan.

in the lab to determine the total amount of dye absorbed. The numerical spectrophotometer results from the array papers can be seen in Table A.3. These results were converted into DUs and interpolated to show the total dye accumulation on the ground from the plume in Figure 5.4b. From the accumulation results it can be clearly seen that the plume was shifted in the negative Y direction. This correlates with a wind shift in the same direction that occurred before the flight test took place.

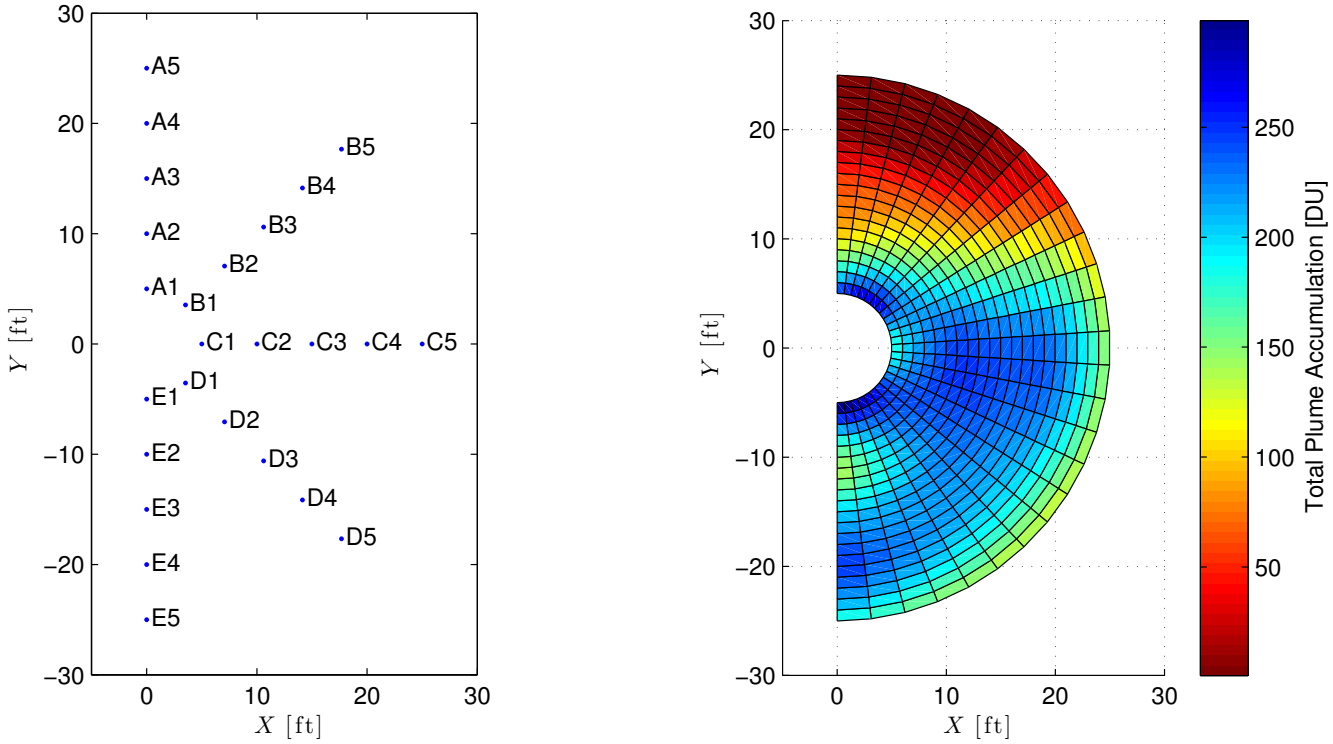

(a) Petri Plate Array Distribution

(b) Dye Accumulation Distribution

Figure 5.4: An array of filter paper samplers arranged as shown in (a) was used to take time averaged samples of the generated plume corresponding to the total dye accumulation on the ground in (b).

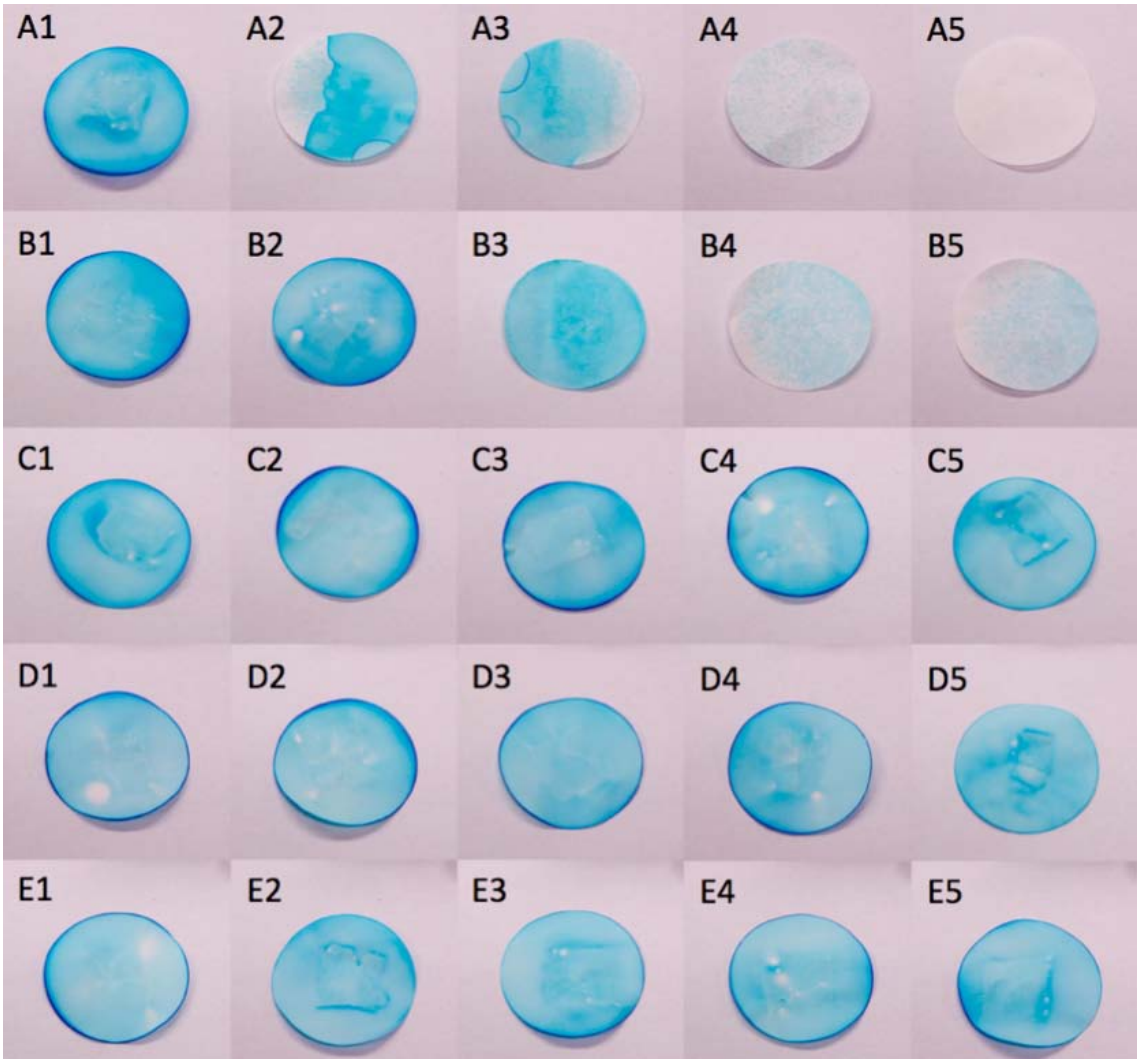

Figure 5.5: Dye was collected by filter papers arranged in an array behind the generated plume in the layout shown in Figure 5.4a. Photos courtesy of Mark C. Palframan.

5.2.2 Sampling

A total of eleven consecutive sampling passes were made through the plume, passing the plume in the upwind direction using a SPAARO UAV[1]. The plume was successfully sampled on the 8$^{\text{th}}$ pass with an airspeed of 112.2 $^{ft}/_{s}$ and a lateral offset of under 2 ft. The successful sampling flight path can be seen in Figure 5.6, where the UAV was flying in a clockwise circuit over the orchard sprayer, which is represented by the blue square. The UAV reached its minimum altitude shortly after passing the orchard sprayer. Information about all flight passes can be found in Appendix B.

Figure 5.7 shows the dye accumulation rate with the sampling flight path overlaid on top. Using these accumulation values as well as the UAVs recorded airspeed, we estimated that the petri samplers would collect 6.19 DU. The actual amounts of dye collected by the filter paper plates, shown directly after the flight test in Figure 5.8, were 7.99 DU from the left plate and 9.67 DU from the right plate. Given that the plume dispersion model is time-averaged and two-dimensional, it does not capture the temporal or vertical variations of dye concentration within the plume. The small error between the actual and predicted dye collection values is reasonable, given these sources of error.

By comparing the amount of dye collected by the petri plate samplers and the impinger, we can calculate the efficiency of the aerial collection system. Taking into account the surface areas of the two collection devices, the amount of liquid sample used, and the airspeed

[1]The SPAARO airframe was flown at Kentland Research Farm with FAA clearance under COA 2011-ESA-64

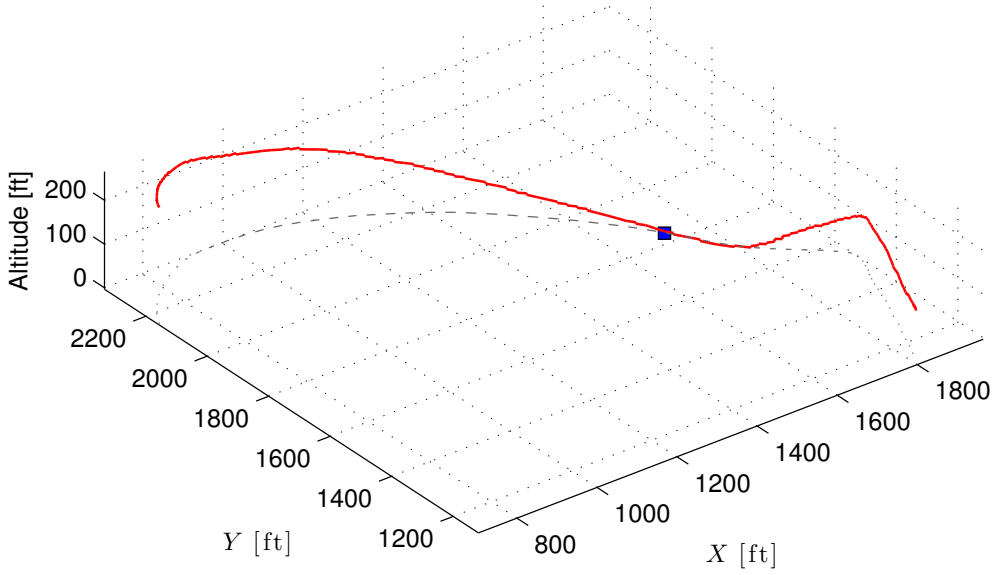

Figure 5.6: SPAARO's successful sampling flight path, shown in red, passed from left to right overtop of the orchard sprayer, marked in blue.

velocities, we can compare the dye densities from the two systems and get an efficiency of 60.81%. For full calculations, see Appendix C.

5.3 Self-Spraying Analyte Flight Test

The SPR sensor was reintegrated into the collection system following the dye plume flight test. The self-spray mechanism was then used with the combined SPR and collection subsystems to perform fully autonomous detections of a self-sprayed analyte first in a ground

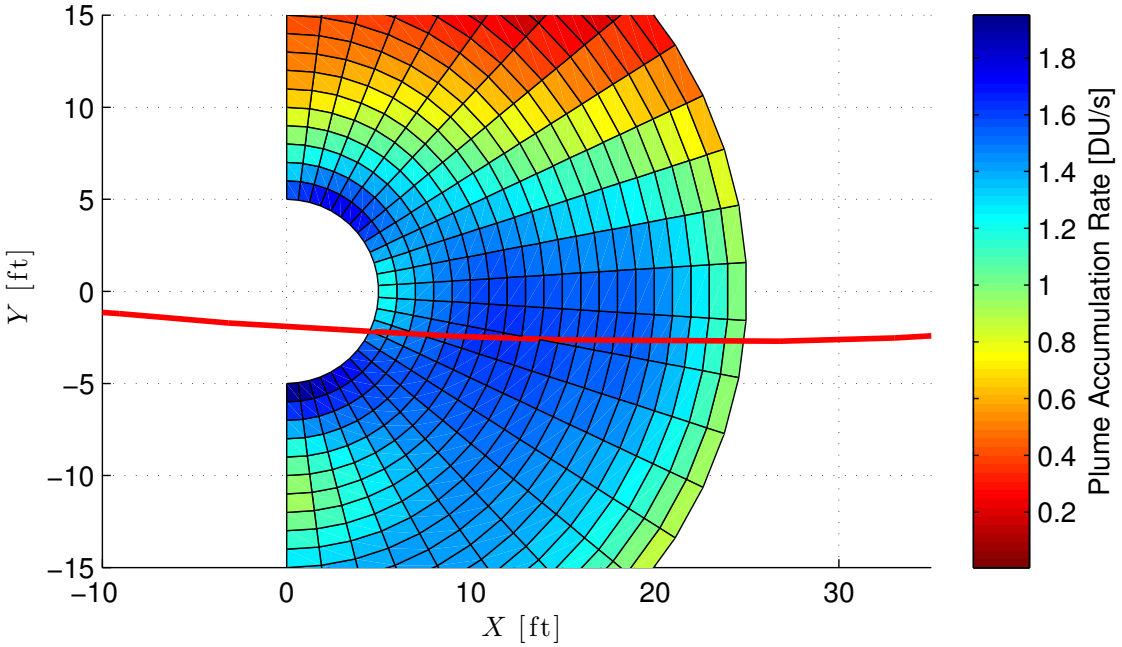

Figure 5.7: The sampling flight path from Figure 5.6 can be seen overlaid on the time averaged dye accumulation rate derived from Figure 5.4b.

test, and subsequently in a flight test.

5.3.1 Ground Test

A 3 *ml* sample of a 50% sucrose solution was sprayed into the collector inlet and subsequently detected by the SPR sensor. 15 *ml* of PBST solution was used in the impinger vial, ideally generating a solution of 8.33% sucrose. Figure 5.9 shows the detection curves of the four Spreeta sensor chips in series in response to the sucrose sample. After being initialized by pure PBST, the signals from the chips were zeroed at 0 seconds on the graph.

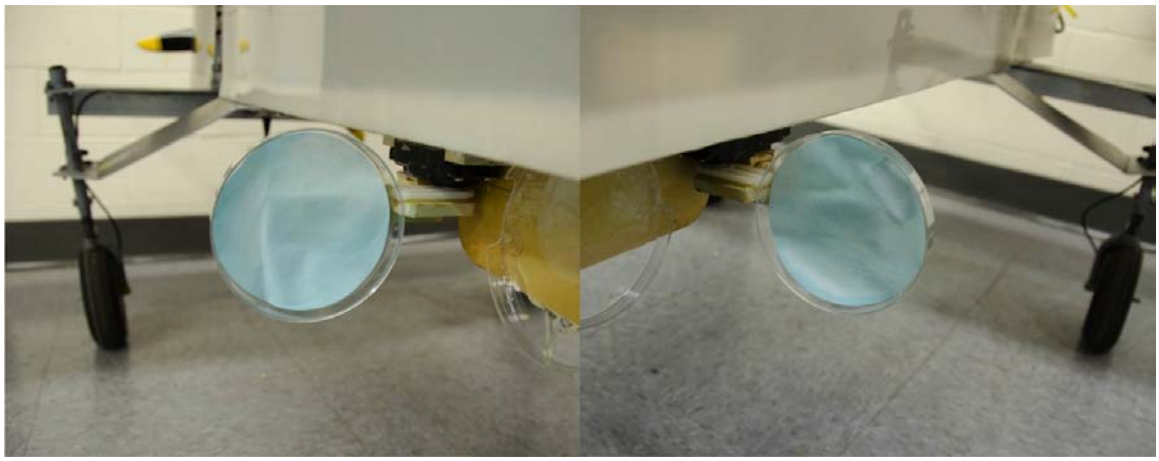

Figure 5.8: SPAARO's two filter paper samples can be seen dyed blue following the successful plume fly through. Photos courtesy of Mark C. Palframan.

The collection system was triggered at 395 seconds and finished 45 seconds later at 440 seconds. At this point the PBSTA had reached the buffer reservoir and the SPIRIT system was pressurized to remove any bubbles. A small jump in the sensor readings can be seen on the graph corresponding to the pressurization point. The sucrose detection spiked at 615 seconds, about 3 minutes after the sample reached the buffer reservoir. The peristaltic pump in the SPIRIT unit was run at 50% of its maximum speed. After spiking, the four sensors reached a steady state of about 2580 RUs. A steep RU drop off can be seen at 935 seconds, corresponding to a commanded flush of the sensor chambers by the SPR groundstation. After the flush, there was no remaining PBSTA in the sensor chambers, but still PBSTA solution in the tubing in between the Spreeta chips and the buffer reservoir. At this point, the PBSTA buffer reservoir was manually switched out and a pure PBST solution was flowed through the sensor chamber, rinsing out any remaining PBSTA solution, and resulting in a second spike where diluted PBSTA reentered the sensor chambers. This was followed by a

decline to zero by all sensor chips as the remaining PBSTA left the system. Sensor 1 showed a steady drift off of the zero point after being initialized and zeroed, which is once again evident between 1100 and 1400 seconds.

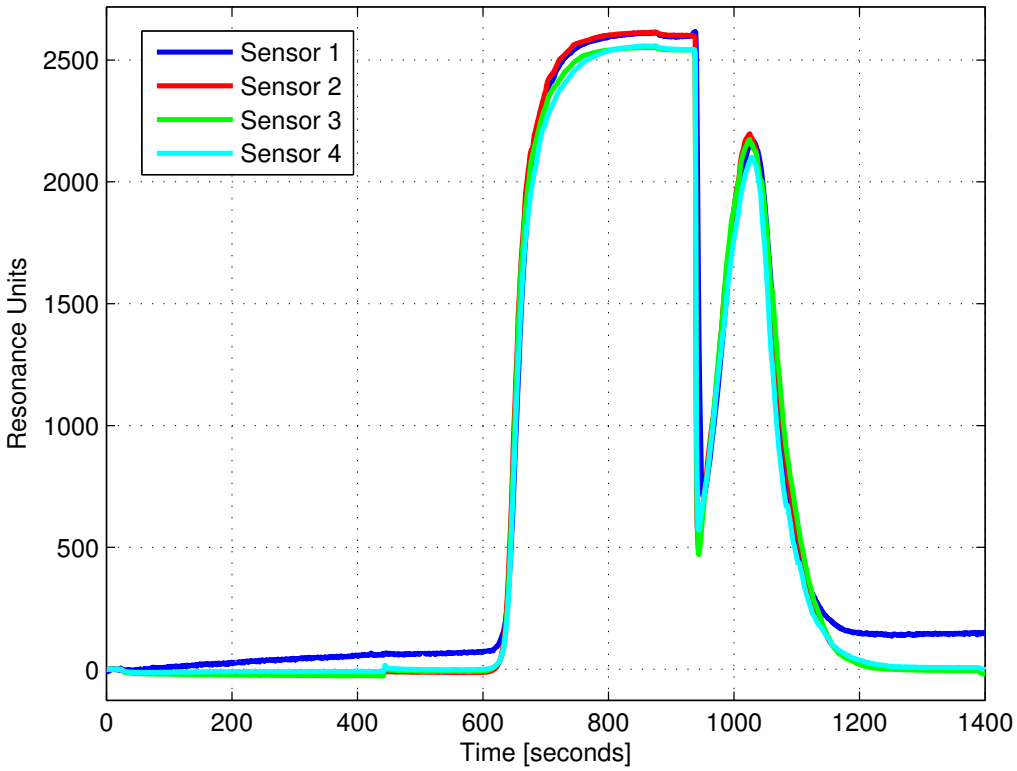

Figure 5.9: A 50% sucrose solution was detected by the SPR sensor during a fully autonomous ground test. Four sensors were used in tandem to detect the sucrose solution, all of which successfully spiked and returned to their initial state after analyte was washed out of the sensor chambers. A steady drift off of the zero point can also be observed in sensor 1.

5.3.2 Flight Test

An aerial version of the previous test was conducted on April 25th, 2013[2]. Once again, $3\,ml$ of 50%/ sucrose solution was sprayed and collected in $15\,ml$ of PBST. The sensor was initialized with PBST and zeroed while on the ground. Following the 45 second autonomous aerial sampling phase, the SPR was pressurized at 175 seconds, once again corresponding to a slight jump in RU, as can be seen in Figure 5.10. The detection spike was observed after eight and a half minutes at 685 seconds, with the peristaltic pump running at 50% capacity. The UAV landed at approximately 500 seconds, about 150 seconds after a detection was expected due to an expected fault in the system due to the prolonged detection time. While the UAV was sitting on the ground, with the onboard systems still acting autonomously, the detection spiked and then peaked at approximately $2885\,RU$. This steady state value is an 11.8% increase from the ground test, and therefore clearly represents a successful detection. The sensor chambers were autonomously flushed at 1500 seconds. The buffer reservoir was then switched out on the ground and pure PBST was run through the system to once again flush out any remaining sucrose and return the sensor chip readings to zero.

5.3.3 Sensor Connectivity

During the 15 minute flight, the groundstation laptop lost connectivity with the SPR sensor four times and had to be manually reconnected by the groundstation operator. Po-

[2]The SPAARO airframe was flown at Kentland Research Farm with FAA clearance under COA 2012-ESA-92

tential reasons for this connection drop include antenna shielding on the UAV end from the aircraft's large metal landing gear, groundstation shielding from vehicles parked near the groundstation site, and range issues from flying too high and far away from the groundstation site. These connection drops may have resulted in the stoppage of the SPR sensor's peristaltic pump during drop times, and potentially not resuming pumping when a new connection was made, which would have resulted in the increased detection time experienced by the SPR system. After removing the ground vehicles, raising up the groundstation antenna, and altering the UAV's flight path to fly closer and lower to the groundstation, no further connectivity issues arose.

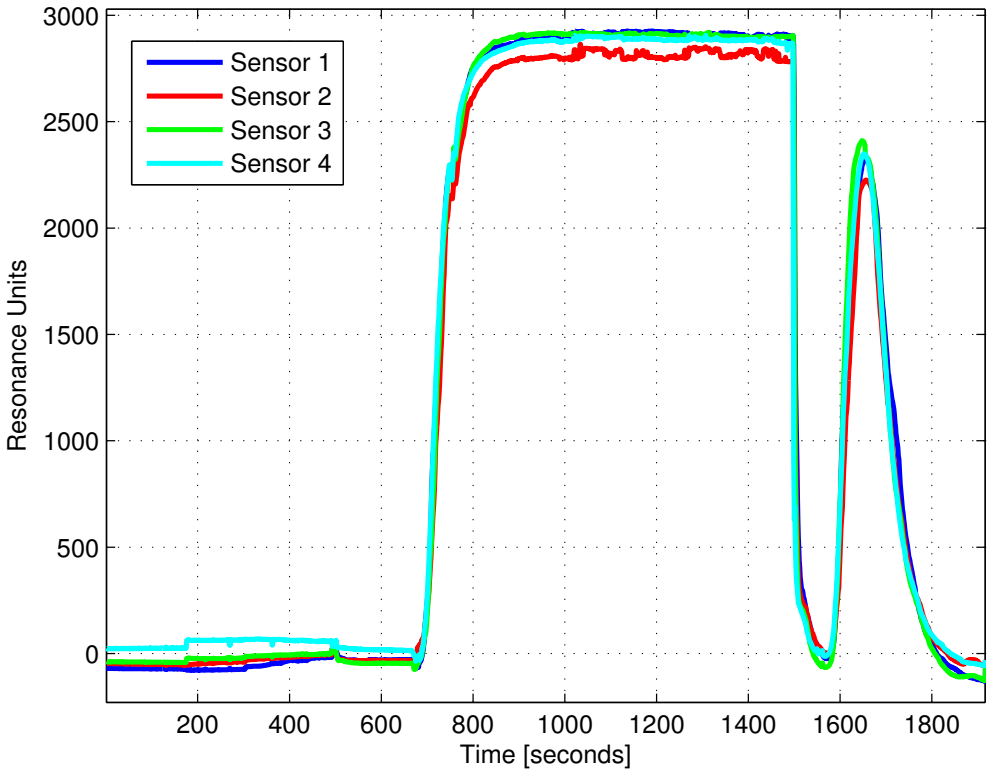

Figure 5.10: A 50% sucrose solution was detected by the SPR sensor during a fully autonomous flight test. Four sensors were used in tandem to detect the sucrose solution, all of which successfully spiked and returned to their initial state after analyte was washed out of the sensor chambers.

Chapter 6

Conclusions and Future Work

An impinger based aerial particle collection system was successfully designed, built and automated in a SPAARO UAV. After being flown through a plume of dye, it was determined that the collection system had an aerial efficiency of 61% with respect to the actual atmospheric concentration. An SPR sensor was then integrated into the collection system, and shown to collect particles with a high enough concentration to be successfully detected by the SPR sensor in ground tests.

In a culminating flight test, the UAV had a successful aerial collection of a sucrose solution sprayed directly in front of the onboard sampling system. After the expected detection period had passed, the UAV landed and shortly thereafter, the sucrose sample was autonomously detected by the SPR sensor, with sensor readings updating in real time on the sensor's groundstation computer.

After a successful proof of concept, the next step is to upgrade the both systems. A more efficient collection system will allow more sparsely distributed analytes to be detected, while an improved fluidics system will allow multiple detections to be made per flight. By designing a cyclone sampling unit similar to the one used by Anderson et al., the minimum concentration detection limit could be lowered [10]. A cyclone sampler would allow for an increased air flow rate into the sampler as well as decrease the amount of liquid required to capture particles. The SPR sensor would therefore receive a sample with an increased sample in buffer concentration with respect to the sample in air concentration.

An upgraded fluidics system would allow the sensor to run multiple detection cycles whilst airborne as well as improve sensor readings. The ability to autonomously run pure PBST as opposed to PBSTA over the Spreeta chips would allow the sensors to be zeroed prior to each detection cycle and whilst airborne. A system to inject amplifier would decrease sensor noise as well as decrease the lower bound detection limit. A regenerative cleaning solution would then be needed to wash the Spreeta chips in order to dissociate the previous analyte and prepare for a new detection. Used PBSTA would need to be pumped out of the buffer reservoir and into a waste container following a detection cycle, at which point fresh buffer would be needed to run the cyclone/impinger for each new detection.

Now that we have ascertained the entire collection/detection system works, the next step is to sample a deactivated biological agent in a self-spray configuration and then from a plume. The self-spraying system will be used to initially test the SPR system due to the expense associated with spraying large quantities of biological agent. By using a SPAARO

airframe equipped with the previously tested aerial spray system, we can generate a smaller, but more directed plume for testing. The sprayer SPAARO and the SPR equipped SPAARO can be flown in coordinated flight in order to ensure collection of the sprayed plume.

A higher power wireless serial connection in addition to a second antenna located on top of the UAV would help to ensure that the SPR sensor maintains connectivity through banked turns and while flying at greater distances from the groundstation. An autonomous system to run the SPR system from the UAV would also reduce performance issues associated with connection drops, and only require the groundstation for viewing detection results.

Appendix A

Raw Data

Table A.1: Raw OD values for UAV petri plate and impinger samples corresponding to Section 5.2.

Sample	Left Petri	Right Petri	Impinger
1	0.374	0.457	0.0140
2	0.378	0.462	0.0411
3	0.373	0.442	0.0410

Table A.2: Raw OD values for for the dye calibration curve presented in Section 4.

	Sample Number		
Units	1	2	3
6	0.290	0.330	0.282
8	0.396	0.382	0.410
10	0.471	0.489	0.481
12	0.604	0.591	0.585
14	0.751	0.764	0.667
16	0.882	0.998	0.872
18	0.908	0.958	0.960
20	1.010	1.018	0.880
22	1.055	1.048	1.088
24	1.173	1.134	1.173
26	1.203	1.180	1.270
28	1.304	1.379	1.335
30	1.503	1.426	1.477
32	1.560	1.485	1.489
34	1.638	1.593	1.554
36	1.597	1.572	1.588
38	1.714	1.718	1.690
40	1.799	1.743	1.763

Table A.3: Raw OD values for petri plate array samples corresponding to Section 5.2.

	Sample Number		
Units	1	2	3
A1	2.125	2.127	0.481
A2	0.870	0.884	0.882
A3	0.592	0.589	0.572
A4	1.006	1.010	1.008
A5	0.075	0.073	0.058
B1	2.479	2.450	2.461
B2	1.298	1.539	1.553
B3	0.779	0.783	0.791
B4	0.220	0.216	0.218
B5	0.173	0.165	0.164
C1	1.754	1.740	1.691
C2	2.270	2.222	2.281
C3	2.190	2.176	2.145
C4	1.987	2.043	2.094
C5	1.137	1.130	1.130
D1	2.300	2.419	2.235
D2	2.180	2.169	2.168
D3	2.138	2.134	1.999
D4	1.849	1.860	1.794
D5	1.075	1.056	1.083
E1	2.840	2.898	2.662
E2	1.325	1.392	1.384
E3	1.933	1.942	1.952
E4	2.332	2.256	2.251
E5	1.545	1.500	1.421

Appendix B

Flight Data

Table B.1: 11 attempted passes were made at sampling the plume of of dye as discussed in Section 5.2. The 8^{th} pass, which can be seen to have the smaller lateral offset from the array centerline, successfully sampled the plume. The airspeeds and relative altitudes from the takeoff height are also shown.

Sample	1	2	3	4	5	6	7	8	9	10	11
Airspeed $[\frac{m}{s}]$	31.9	35.3	34.2	35.3	34.7	33.3	33.1	34.2	31.9	33.3	31.9
Altitude $[m]$	4	7	5	5	1	2	2	1	0	0	0
Lateral $[m]$	-11.1	-10.5	-5.79	-12.5	3.68	-6.22	3.45	0.56	-5.89	-8.01	-1.94

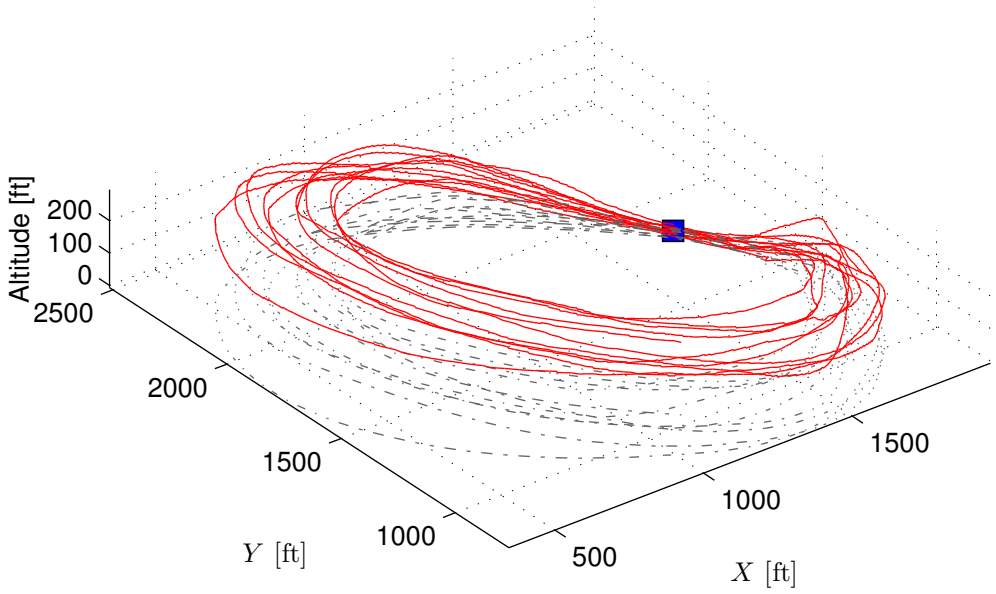

Figure B.1: The manual sampling passes are shown in red. The blue square represents the orchard sprayer, where the UAV was flying from left to right over the sprayer with respect to the figure.

Table B.2: The mean airspeed, altitude, and lateral offset distance are shown for all of the sampling passes discussed in Section 5.2

	μ	σ	σ^2
Airspeed $[\frac{m}{s}]$	33.56	2.45	-4.93
Altitude $[m]$	1.27	2.42	5.67
Lateral $[m]$	1.62	5.87	32.18

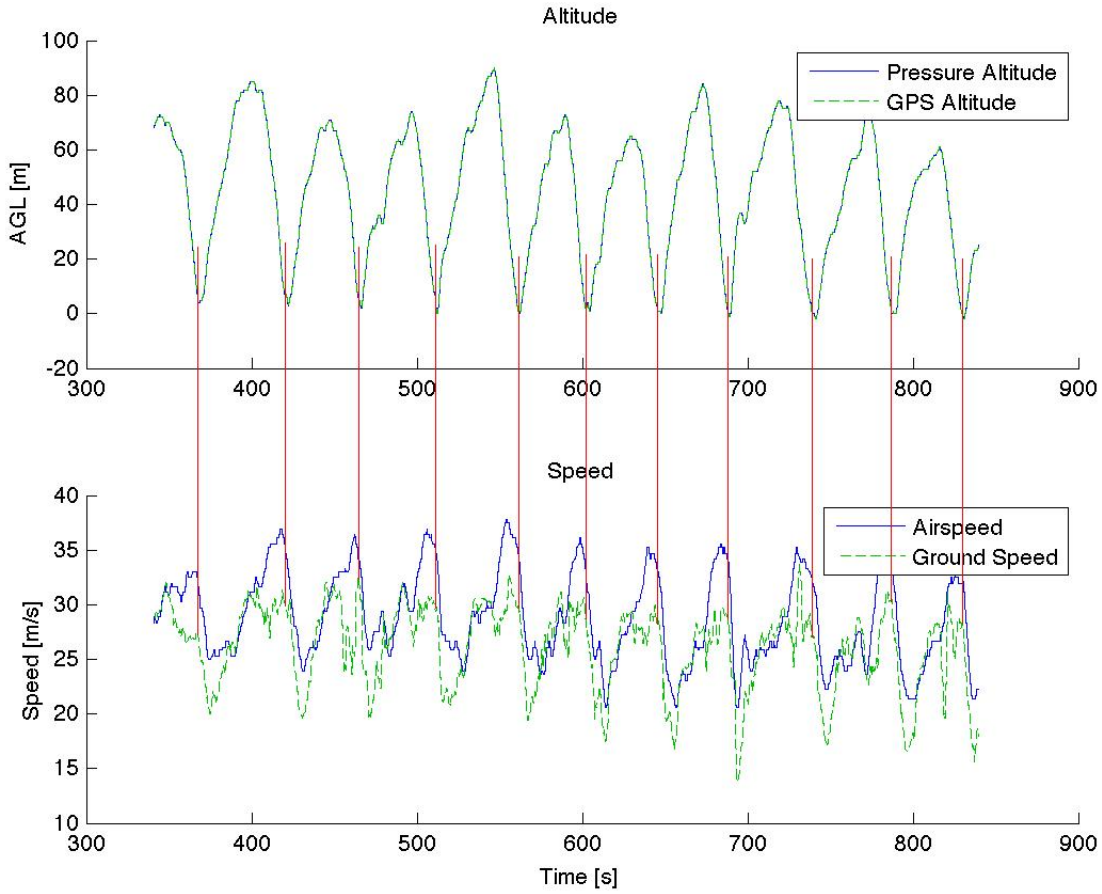

Figure B.2: Altitude and speed measurements from the flight activities in Section 5.2 are shown. The locations passing over the dye plume are marked with vertical red lines.

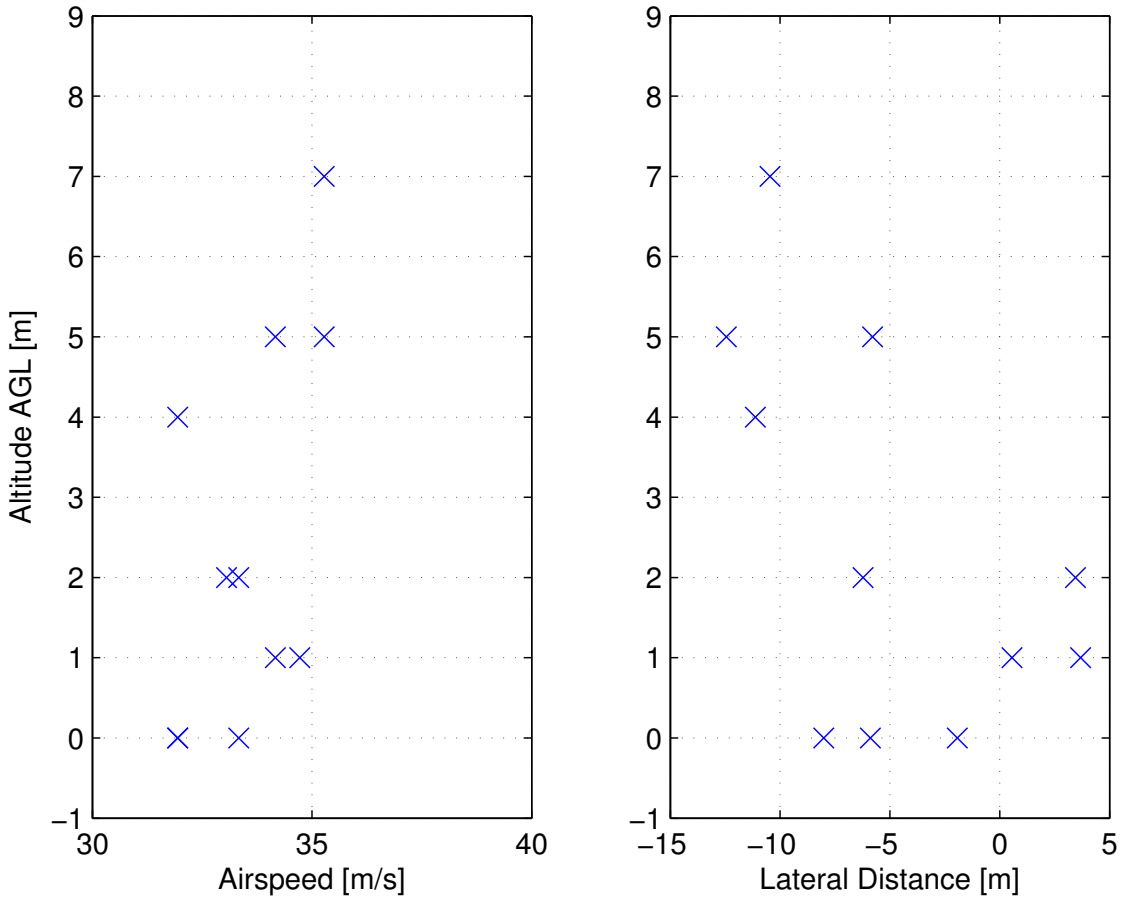

Figure B.3: The lateral offset, altitude, and airspeed of sampling passes are presented below. Note that the orchard sprayer was located at a slightly lower elevation than the runway where altitude was initialized.

Appendix C

Efficiency Calculations

A_i, A_p	Frontal collection area
d_i, d_p	Collection diameter
D_i, D_p	Dye density
DU_i, DU_p	Amount of dye units
V_i, V_p	Volume of liquid sample
V_∞, V_f	Airspeed / fan velocity

Impinger Calculations

$V_\infty = 1346.45\,{}^{in}/_{s}$

$V_f = 264.57\,{}^{in}/_{s}$

$V_i = 20\,ml$

$d_i = 1.5\,in$

Impinger collection tube area was calculated

$A_i = \pi\frac{d_i^2}{4} = 1.767\,in^2$

Average Optical Density value for the impinger was calculated

$OD_i = \frac{0.0140+0.0141+0.0140}{3} = 0.01407\,{}^{RU}/_{mL}$

Values were converted to Dye Units

$DU_i = \frac{OD_i}{0.0469\,{}^{DU\,mL}/_{RU}} V_i = 5.99\,DU$

Values were converted to Dye Units per volumetric flow rate

$D_i = \frac{DU_i}{A_i(V_\infty + V_f)} = 2.107 \times 10^{-3}\,{}^{DU\,s}/_{in^3}$

Petri Plate Calculations

$V_p = 5\,ml$

$d_p = 3.5\,in$

Petri plate sampler area was calculated

$A_p = \pi\frac{d_p^2}{4} = 9.621\,in^2$

Average Optical Density value for the petri plates was calculated

$OD_p = \frac{0.374+0.378+0.373+0.457+0.462+0.442}{6} = 0.414\,{}^{RU}/_{mL}$

Values were converted to Dye Units

$DU_p = \frac{OD_p}{0.0469\,{}^{DU\,mL}/_{RU}} V_i = 44.17\,DU$

Values were converted to Dye Units per volumetric flow rate

$D_p = \frac{DU_p}{A_p V_\infty} = 3.409 \times 10^{-3}\,{}^{DU\,s}/_{in^3}$

Efficiency

$\epsilon = 100\frac{D_i}{D_p} = 60.807\%$

Appendix D

Arduino Code

D.1 Dye Plume Flight Test

/*Arduino Board Layout - counterclockwise from top:

1 - Main power

2 - Fan Power

3 - Servo Power

4 - Spray

5 - Wash

6 - Move

7 - Fan

8 - Left Sampler

9 - Right Sampler

10 - SPR Servo

11 - Receiver Input

*/

```
#include <Servo.h>
Servo sampler;
Servo sampler2;
Servo SPR;
int sprOpen = 115;
int sprClosed = 65;
int sOpen = 55;
int sClosed = 128;
int s2Open = 110;
int s2Closed = 39;
int receiverPin = 2;
int movePin = 51;
int sprayPin = 39;
int washPin = 37;
int fanPin = 49;
int anPin = 1;
long int duration = 1;
long int startTime = 0;
long int voltage = 0;
boolean runSPR = false;
boolean ready = true;
boolean collecting = true;
// the setup routine runs once when you press reset:
void setup() {
    // initialize the digital pin as an output.
    pinMode(movePin, OUTPUT);
    pinMode(washPin, OUTPUT);
    pinMode(receiverPin, INPUT);
```

```
    pinMode(fanPin, OUTPUT);
    pinMode(22, OUTPUT);
    SPR.attach(9);
    sampler.attach(12);
    sampler2.attach(13);
    Serial.begin(57600);
    //
    //Initialization of system
    sampler.write(sClosed);
    sampler2.write(s2Closed);
    SPR.write(sprClosed);
    digitalWrite(movePin, LOW);
    digitalWrite(washPin, LOW);
    digitalWrite(fanPin, LOW);
}
// the loop routine runs over and over again forever:
void loop() {
    while (ready){
        //duration=pulseIn(receiverPin,HIGH);
        voltage=analogRead(anPin);
        Serial.println(voltage);
        if (voltage>900 && ready==true){
            runSPR=true;
        }
        if (runSPR==true && voltage>900){
            runSPR=false;
            while(collecting){
                SPR.write(sprOpen);
```

```
                    sampler.write(sOpen);
                    sampler2.write(s2Open);
                    digitalWrite(fanPin, HIGH);
                    delay(12000);
                    digitalWrite(washPin, HIGH);
                    delay(5000);
                    SPR.write(sprClosed);
                    sampler.write(sClosed);
                    sampler2.write(s2Closed);
                    digitalWrite(fanPin, LOW);
                    digitalWrite(washPin, LOW);
                    delay(2000);
                    collecting=false;
                    ready = true;
                }
                runSPR = false;
                collecting = true;
            }
        }
}
```

D.2 Self-Spray Flight Test

```
/*Arduino Board Layout - counterclockwise from top:
1 - Main power
2 - Fan Power
3 - Servo Power
4 - N/A
5 - Wash
6 - Move
7 - Fan
8 - N/A
9 - Spray
10 - SPR Servo
11 - Receiver Input
*/
#include <Servo.h>
Servo sampler;
Servo sampler2;
Servo SPR;
int sprOpen = 115;
int sprClosed = 65;
int sprayStart = 128;
int sprayEnd = 79;
int receiverPin = 2;
int movePin = 51;
int washPin = 37;
int fanPin = 49;
int anPin = 1;
long int duration = 1;
```

```
long int startTime = 0;
long int voltage = 0;
boolean runSPR = false;
boolean ready = true;
boolean collecting = true;
// the setup routine runs once when you press reset:
void setup() {
    // initialize the digital pin as an output.
    pinMode(movePin, OUTPUT);
    pinMode(washPin, OUTPUT);
    pinMode(receiverPin, INPUT);
    pinMode(fanPin, OUTPUT);
    pinMode(22, OUTPUT);
    SPR.attach(9);
    spray.attach(12);
    Serial.begin(57600);
    //
    //Initialization of system
    spray.write(sprayStart);
    SPR.write(sprClosed);
    digitalWrite(movePin, LOW);
    digitalWrite(washPin, LOW);
    digitalWrite(fanPin, LOW);
}
// the loop routine runs over and over again forever:
void loop() {
    while (ready){
        //duration=pulseIn(receiverPin,HIGH);
```

```
voltage=analogRead(anPin);
Serial.println(voltage);
if (voltage>900 && ready==true){
    runSPR=true;
}
if (runSPR==true && voltage>900){
    runSPR=false;
    while(collecting){
        SPR.write(sprOpen);
        spray.write(sprayStart);
        digitalWrite(fanPin, HIGH);
        spray.write(sprayEnd);
        delay(5000);
        digitalWrite(washPin, HIGH);
        delay(5000);
        SPR.write(sprClosed);
        digitalWrite(fanPin, LOW);
        digitalWrite(washPin, LOW);
        delay(2000);
        digitalWrite(movePin, HIGH);
        delay(5000);
        digitalWrite(movePin, LOW);
        collecting=false;
        ready = true;
    }
    runSPR = false;
    collecting = true;
}
```

```
    }
}
```

Bibliography

[1] Aylor, D. E., Schmale, D. G., Shields, E. J., Newcomb, M., and Nappo, C. J., "Tracking the potato late blight pathogen in the atmosphere using unmanned aerial vehicles and Lagrangian modeling," *Agricultural and Forest Meteorology*, Vol. 151, No. 2, Feb. 2011, pp. 251–260.

[2] Ligler, F. S., Anderson, G. P., Davidson, P. T., Foch, R. J., Ives, J. T., King, K. D., Page, G., Stenger, D. A., and Whelan, J. P., "Remote Sensing Using an Airborne Biosensor," *Environmental Science & Technology*, Vol. 32, No. 16, Aug. 1998, pp. 2461–2466.

[3] Schmale, D. G., Dingus, B. R., and Reinholtz, C., "Development and Application of an Autonomous Unmanned Aerial Vehicle for Precise Aerobiological Sampling above Agricultural Fields," *Journal of Field Robotics*, Vol. 25, No. 3, 2008, pp. 133–147.

[4] O'Brien, T., Johnson, L. H., Aldrich, J. L., Allen, S. G., Liang, L. T., Plummer, A. L., Krak, S. J., and Boiarski, A. A., "The Development of Immunoassays to Four Biological Threat Agents in a Bidiffractive Grating Biosensor," *Biosensors & bioelectronics*, Vol. 14, No. 10-11, Jan. 2000, pp. 815–28.

[5] Rogers, K. R. and Lin, J. N., "Biosensors for Environmental Monitoring," *Biosensors and Bioelectronics*, Vol. 7, No. 5, Jan. 1992, pp. 317–321.

[6] Koch, S., Wolf, H., Danapel, C., and Feller, K. A., "Optical Flow-Cell Multichannel Immunosensor for the Detection of Biological Warfare Agents." *Biosensors & bioelectronics*, Vol. 14, No. 10-11, Jan. 2000, pp. 779–84.

[7] Wein, L. M., Craft, D. L., and Kaplan, E. H., "Emergency response to an anthrax attack." *Proceedings of the National Academy of Sciences of the United States of America*, Vol. 100, No. 7, April 2003, pp. 4346–51.

[8] Yu, H., Raymonda, J. W., McMahon, T. M., and Campagnari, A. A., "Detection of Biological Threat Agents by Immunomagnetic Microsphere-Based Solid Phase Fluorogenic- and Electro-Chemiluminescence," *Biosensors & Bioelectronics*, Vol. 14, 2000, pp. 829–840.

[9] Rowe, C. A., Tender, L. M., Feldstein, M. J., Golden, J. P., Scruggs, S. B., Maccraith, B. D., Cras, J. J., and Ligler, F. S., "Array Biosensor for Simultaneous Identification of Bacterial , Viral , and Protein Analytes," *Analytical Chemistry*, Vol. 71, No. 17, 1999, pp. 3846–3852.

[10] Anderson, G. P., King, K. D., Cuttino, D. S., Whelan, J. P., Ligler, F. S., MacKrell, J. F., Bovais, C. S., Indyke, D. K., and Foch, R. J., "Biological Agent Detection with the Use of an Airborne Biosensor," *Field Analytical Chemistry & Technology*, Vol. 3, No. 4-5, 1999, pp. 307–314.

[11] Naimushin, A. N., Spinelli, C. B., Soelberg, S. D., Mann, T., Stevens, R. C., Chinowsky, T. M., Kauffman, P., Yee, S. S., and Furlong, C. E., "Airborne Analyte Detection with an Aircraft-Adapted Surface Plasmon Resonance Sensor System," *Sensors and Actuators B: Chemical*, Vol. 104, No. 2, Jan. 2005, pp. 237–248.

[12] Liedberg, B., Nylander, C., and Lundstrom, I., "Surface Plasmon Resonance for Gas Detection and Biosensing," *Sensors and Actuators*, Vol. 4, 1983, pp. 299–304.

[13] Roh, S., Chung, T., and Lee, B., "Overview of the Characteristics of Micro- and Nano-Structured Surface Plasmon Resonance Sensors." *Sensors (Basel, Switzerland)*, Vol. 11, No. 2, Jan. 2011, pp. 1565–88.

[14] Wilson, W. D., "Analyzing Biomolecular Interactions," *Science*, Vol. 295, No. 5562, 2002, pp. 2103–2105.

[15] Chinowsky, T. M., Soelberg, S. D., Baker, P., Swanson, N. R., Kauffman, P., Mactutis, A., Grow, M. S., Atmar, R., Yee, S. S., and Furlong, C. E., "Portable 24-Analyte Surface Plasmon Resonance Instruments for Rapid, Versatile Biodetection," *Biosensors and Bioelectronics*, Vol. 22, 2007, pp. 2268–2275.

[16] Cotting, M. C., Murtha, J. F., Techy, L., and Woolsey, C. A., "Examples of Augmentation of an Atmospheric Flight Mechanics Curriculum using UAVs ," *27th AIAA Atmospheric Flight Mechanics Conference and Exhibit*, Chicago, Illinois, 2009.

[17] Cotting, M. C., Wolek, A., Murtha, J. F., and Woolsey, C. A., "Developmental Flight Testing of the SPAARO UAV," *48th AIAA Aerospace Sciences Meeting and Exposition*, Orlando, Florida, 2010.

[18] Murtha, J. F., Cotting, M. C., Wolek, A., Aarons, T., and Woolsey, C. A., "The Educational Impact of Creating a New UAV for Curriculum Enhancement ," *27th AIAA Atmospheric Flight Mechanics Conference and Exhibit*, Chicago, Illinois, 2009.

[19] Techy, L., *Flight Vehicle Control And Aerobiological Sampling Applications*, Dissertation, Virginia Polytechnic Institute and State University, 2009.

[20] Techy, L., Paley, D. A., and Woolsey, C. A., "Unmanned Aerial Vehicle Coordination on Closed Convex Paths in Wind," *Journal of Guidance, Control, and Dynamics*, Vol. 33, No. 6, Nov. 2010, pp. 1946–1951.

[21] Wang, J., Patel, V., Woolsey, C. A., Hovakimyan, N., and Schmale, D. G., "L1 Adaptive Control of a UAV for Aerobiological Sampling," *2007 American Control Conference*, July 2007, pp. 4660–4665.